



Denudation history of the Malawi and Rukwa Rift flanks (East African Rift System) from apatite fission track thermochronology

PETER VAN DER BEEK,^{1,5} EVELYNE MBEDE,² PAUL ANDRIESSEN³
and DAMIEN DELVAUX⁴

¹Laboratoire de Géodynamique des Chaînes Alpines, Institut Dolomieu,
15 rue Maurice Gignoux, 38031 Grenoble cedex, France

²Department of Geology, University of Dar-es-Salaam, Box 35052,
Dar-es-Salaam, Tanzania

³Faculty of Earth Sciences, Vrije Universiteit, De Boelelaan 1085,
1081 HV Amsterdam, the Netherlands

⁴Royal Museum for Central Africa, Steenweg op Leuven 13,
B3080 Tervuren, Belgium

Abstract—Thirty apatite fission track ages and 22 track length measurements are presented from samples of basement rocks flanking the Malawi and Rukwa Rifts (East African Rift System) in order to elucidate the thermotectonic history of the rift flanks. The apatite fission track ages fall in the range 30 ± 15 to 296 ± 10 Ma. The relatively short (11.0–13.2 μm) mean track lengths and wide (1.3–2.3 μm) track length distributions suggest a protracted cooling history for the region, spanning Permian (Karoo) to Recent times. Thermal history reconstruction by inverse model calculations of the track length distribution suggests repeated phases of rapid cooling and denudation of the rift flanks at 250–200 Ma, ~ 150 Ma and ≤ 40 –50 Ma. These appear to be linked to the different rifting events in the area and can be correlated with deposition of the different sedimentary units within the basins. Erosion and isostatic rebound have modified the tectonically induced topography around the rifts: the elevation of the footwall flanks is augmented by flexural isostatic rebound, whereas the topography of the hanging wall flanks has been lowered by erosion. The footwall escarpments of the Malawi and Rukwa rifts are erosional features. The highly elevated plateaus flanking the Western Rift represent an erosional surface traditionally referred to as the “Gondwana surface”. The apatite fission track results of this study suggest that initial exhumation of the “Gondwana surface” to temperatures around 60–70°C took place during Karoo times, but that sub-aerial exposure of the surface did not take place until at least the Early Tertiary. © 1998 Elsevier Science Limited.

Résumé—Nous présentons 30 âges de traces de fission sur apatite et 22 mesures de longueur de trace de fission pour des échantillons du socle dans les flancs des rifts de Malawi et Rukwa (rift est-africain), dans le but de reconstituer l'histoire thermo-tectonique des flancs de ces rifts. Les relativement courtes longueurs moyennes (11.0–13.2 μm) et larges distributions (1.3–2.3 μm) des traces de fission suggèrent un refroidissement prolongé pour la région, allant du Permien (Karoo) à la période récente. La reconstruction de l'histoire thermique par modélisation inverse de la distribution des longueurs de trace de fission suggère que des phases répétées de refroidissement rapide et de dénudation des flancs de rift se sont succédées à 250–200 Ma, ~ 150 Ma et ≤ 40 –50 Ma. Il apparaît qu'elles sont reliées à différentes

⁵Present address: Laboratoire de Géodynamique des Chaînes Alpines, Institut Dolomieu, 15 rue Maurice Gignoux, 38031 Grenoble cedex, France

phases de riftogenèse connues dans la région, et qu'elles peuvent être corrélées avec le dépôt de différentes unités sédimentaires dans les bassins. L'érosion et le réajustement isostatique qui s'en suivit ont modifié la topographie induite par la tectonique autour du rift: l'élévation du compartiment inférieur (footwall flank) est augmentée du rebond isostatique flexural, tandis que la topographie du compartiment supérieur (hangingwall flank) a été abaissée par érosion. Les escarpements du compartiment inférieur des rifts de Malawi et Rukwa sont d'origine érosionnel. Les plateaux élevés bordant la branche occidentale du rift est-africain représentent une surface d'érosion traditionnellement appelée "Surface gondwana". Nos résultats suggèrent que l'exhumation initiale de la "Surface gondwana" à des températures de 60-70°C a eu lieu durant la période Karoo, mais que l'exposition sub-aérienne de cette surface ne s'est pas produite avant au moins le Tertiaire inférieur. © 1998 Elsevier Science Limited.

(Received 25 November 1996: revised version received 28 August 1997)

INTRODUCTION

The East African Rift System has, throughout this century, been considered as a classical area for the study of continental extension. The Western Branch of the East African Rift System, or Western Rift, has been the topic of numerous studies over the last decade alone, which provided many details about the stratigraphy, kinematics and chronology of rifting (e.g. Rosendahl, 1987; Tiercelin *et al.*, 1988; Chorowicz, 1990; Ebinger *et al.*, 1987, 1989, 1993; Delvaux *et al.*, 1992; Ring *et al.*, 1992; Rosendahl *et al.*, 1992; Wheeler and Karson, 1989). In contrast, the uplift history of the rift flanks has so far been less constrained, mainly because of the lack of stratigraphical markers; the flanks expose Precambrian basement rocks. The uplift and denudation history of the region has traditionally been studied in a framework of cyclical geomorphic evolution, with much emphasis being put on the recognition of erosion surfaces of regional to continental extent (e.g. Dixey, 1937, 1947; King, 1963). Although the importance of denudation in creating the present-day morphology of the East African Rift flanks was recognised by early workers (e.g. Dixey, 1947), the elevation of the flanks has, in general, been directly tied to tectonic uplift during Late Cenozoic rifting (e.g. Ebinger *et al.*, 1991, 1993).

During the last decade, apatite fission track (AFT) thermochronology has emerged as a powerful technique to unravel the denudation history of regionally elevated basement regions, because of its ability to constrain the low temperature (< 120°C) cooling history of rock samples (e.g. Foster and Gleadow, 1993; Fitzgerald, 1994; Brown *et al.*, 1994). In this study, AFT analyses of 30 samples collected in recent years from the flanks of the Malawi (Nyasa) and Rukwa Rifts are presented in order

to assess the denudation history of these regions. The AFT data reveal distinct periods of cooling, coincident with extensional phases within the Western Rift. The data also show that the tectonic topography induced by Cenozoic rifting has been modified by erosion. Finally, this paper will show that the summits of the Livingstone Mountains and the eastern flank of the Rukwa Rift define the same structural level, but their denudation history is inconsistent with the Jurassic age that was previously assigned to this surface.

PHYSIOGRAPHIC AND TECTONIC SETTING OF THE WESTERN RIFT

The Western Rift is part of the East African Rift System (EARS), which runs from the Red Sea in the north down to the Zambezi River mouth in Mozambique to the south (Fig. 1, inset). The Western Rift (or Western Branch of the EARS) is segmented into a number of deep and narrow half-graben, often with alternating polarity (Bosworth, 1985; Rosendahl, 1987; Ebinger *et al.*, 1987; Ebinger, 1989). The extensional basins of the Western Rift show distinct and highly elevated rift flanks. Each half-graben is associated with a clearly defined depocentre and a highly uplifted footwall flank; the ramping side of the basins show less topographic elevation. The topography generally rises to over 2 km a.s.l. on the footwall side of the basins adjacent to the border faults, whereas the elevation difference on the ramping sides amounts to some hundreds of metres, enhancing basin asymmetry (Ebinger, 1989).

Although the Malawi Rift lies south of the Mbeya region, where the Eastern and Western Branches of the EARS intersect (Figs 1 and 2), it is usually considered as part of the Western

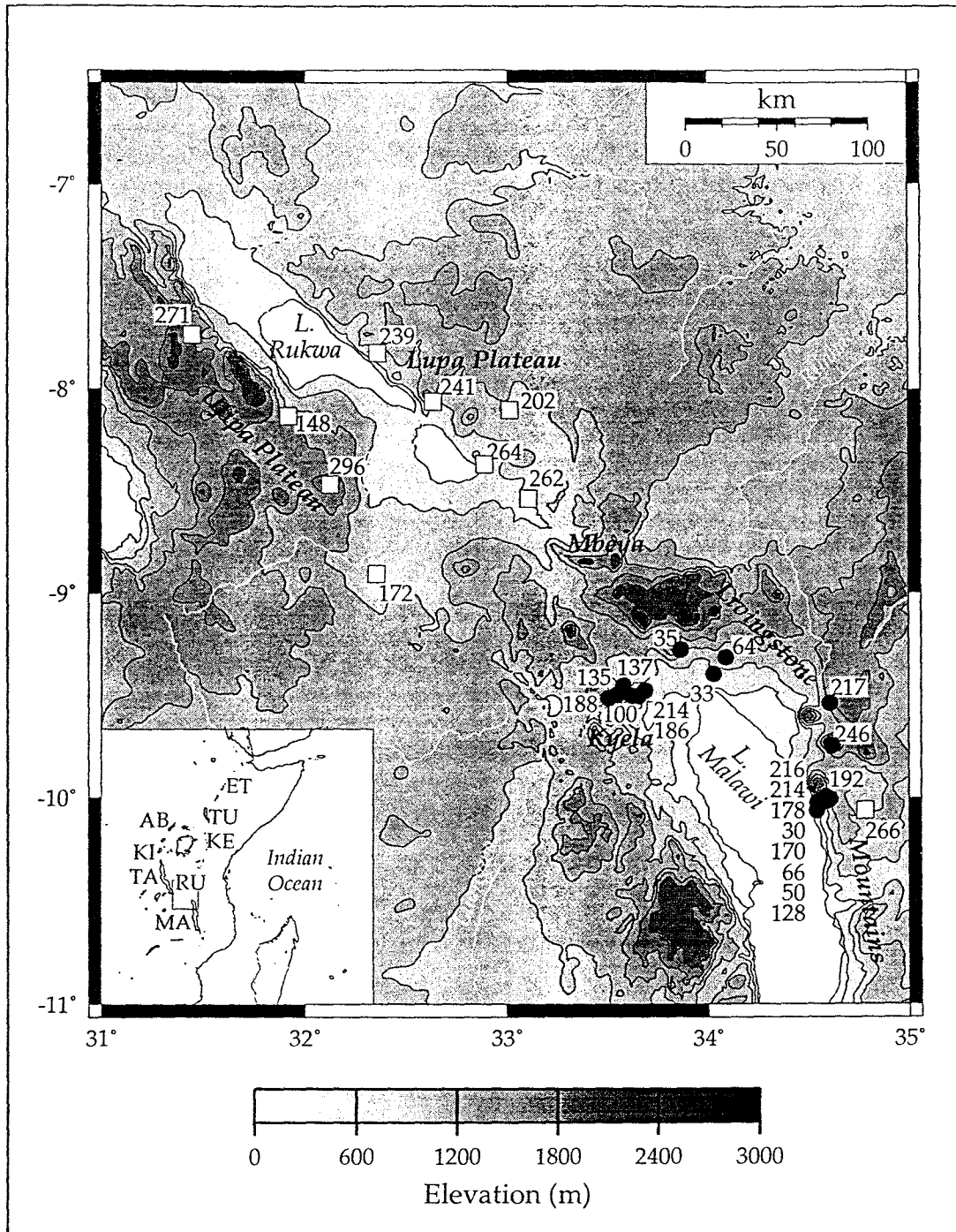


Figure 1. Topographic map of the Malawi-Rukwa Rift region, constructed from the USGS gtopo-30 database (30" resolution; here reproduced at 1'), showing the distribution of apatite fission track samples for this study. Samples are indicated by their AFT age; ●: analysed by van der Beek (1995); □: samples from Mbede et al. (1993). Inset shows location of the study area on the African continent; strings of lakes outline the position of the East African Rift branches: AB: Albert; KI: Kivu; TA: Tanganyika; RU: Rukwa; MA: Malawi (Western Branch); ET: Ethiopian; TU: Turkana; KE: Kenya (Eastern Branch).

Rift because of its structural similarities with the other rift basins in this branch (e.g. Rosendahl, 1987; Rosendahl *et al.*, 1992). The eastern (footwall) flank of the northernmost part of the Malawi Rift rises up to 2.0 km above the present

lake level, forming the Livingstone Mountains, whereas the elevation of the ramping side of the basin is approximately 1.5 km above the present lake level (Fig 1). The Livingstone Mountains are bounded by the Livingstone

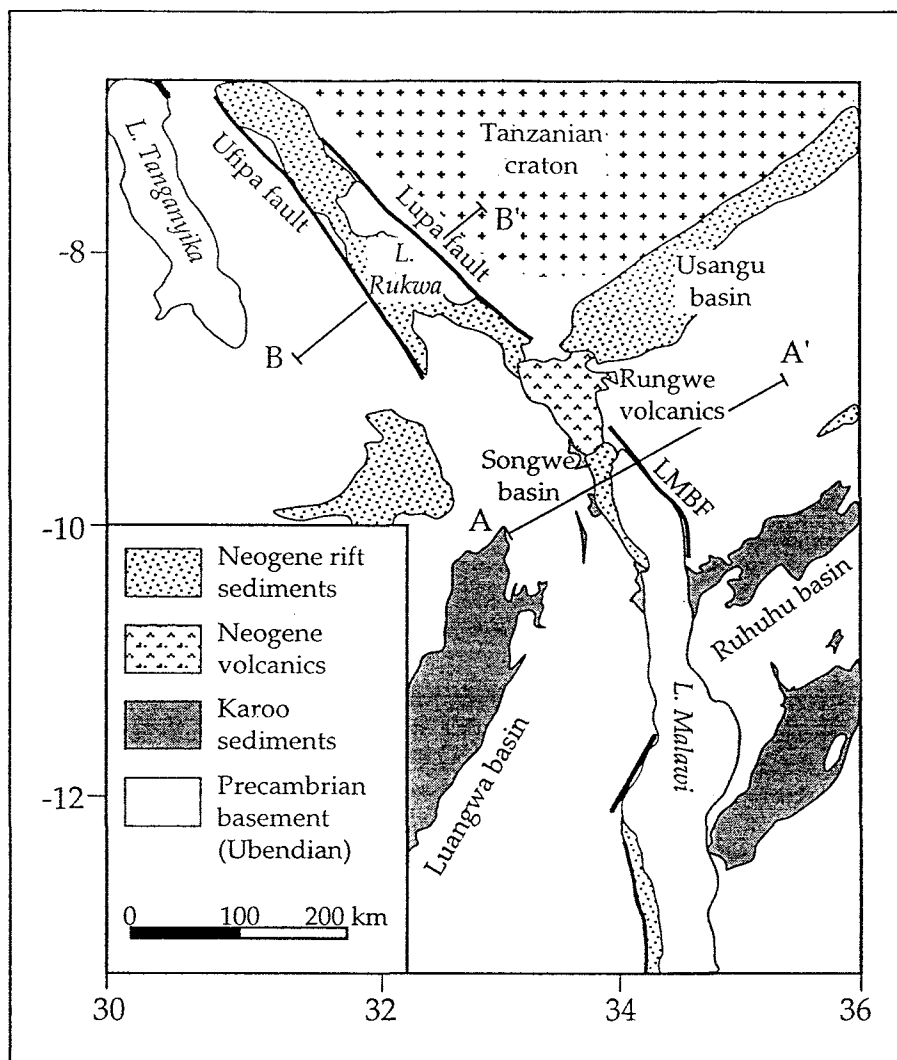


Figure 2. Simplified geological map of the study region. A-A' is the profile across the Malawi Rift depicted in Figs 9 and 10; B-B' is the profile across the Rukwa Rift shown in Fig. 11.

Mountains Border Fault (LMBF) but the Livingstone Mountains Escarpment appears to be at least partly erosional in origin (Dixey, 1947). The summit of the mountains defines an erosional plateau, thought to be a remnant of the Jurassic "Gondwana surface" (King, 1963; Delvaux and Wopfner, 1992). The morphology of the Rukwa Rift provides an exception to the general pattern; here the flank adjacent to the Lupa Border Fault is elevated by less than 400 m with respect to lake level, whereas the opposite flank (the Ufipa Plateau) rises more than 1000 m above the surrounding topography (Mbede, 1993).

The oldest rock units flanking the Western Rift within the Rukwa-Malawi zone (Fig. 2) are the basement rocks of the Ubendian system, composing granitic gneisses, paragneisses, migmatites, metadolerites and amphibolites

(Harkin, 1955). The age of metamorphism of the Ubendian rocks is placed between 2100-1700 Ma (Lenoir *et al.*, 1994); the last Precambrian thermal activity recorded in the region is the older Pan-African tectonothermal event, at *ca* 750 Ma (Theunissen *et al.*, 1992; U-Pb on zircon).

Three Phanerozoic episodes of extension and basin filling are recognised in the Western Rift: the Karoo rifting event (Permo-Triassic), a Late Mesozoic-Cenozoic phase, and Late Cenozoic-Recent rifting. During these periods, rifting was concentrated in coinciding zones, which were strongly controlled by the pre-existing basement structures (Daly *et al.*, 1989; Versfelt and Rosendahl, 1989; Theunissen *et al.*, 1996). The border faults of the Rukwa and Malawi Rifts are superimposed on major Pan-African shear zones which separate the Tanzanian Craton from the Zambian and central African Cratons.

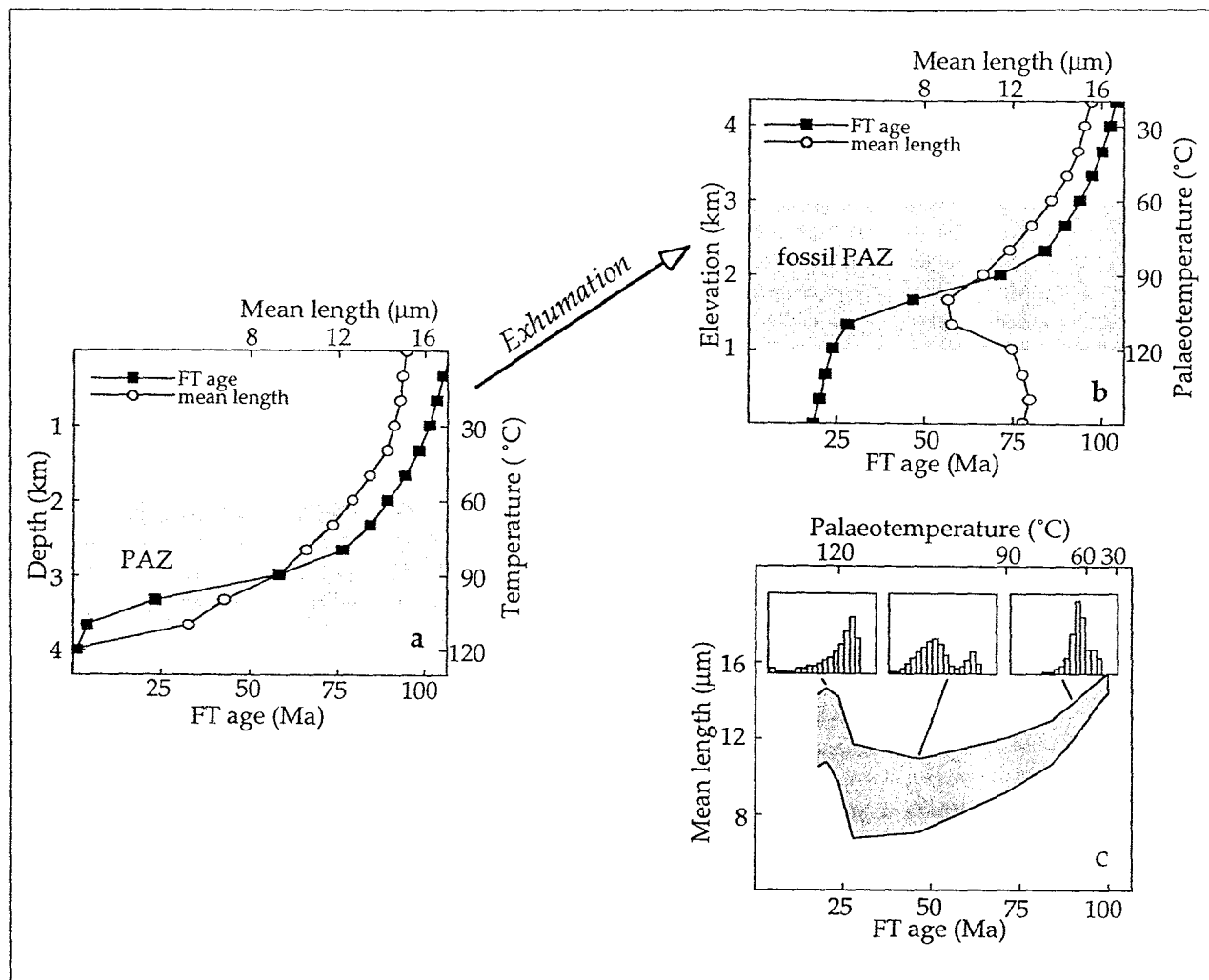


Figure 3. (a) Variation of fission track age and mean track length with temperature, calculated using the annealing model of Laslett *et al.* (1987), for a 100 Ma stable thermal regime. A depth scale is added assuming a $30^{\circ}\text{C km}^{-1}$ geotherm and 0°C surface temperature. Both fission track age and mean track length decrease rapidly between $\sim 60\text{--}120^{\circ}\text{C}$ in the partial annealing zone (PAZ). (b) Pattern of fission track ages and mean track lengths with elevation after 5 km of uplift and denudation from 25 Ma onward. The base of the fossil PAZ is characterised by a break in slope in the age-elevation plot and records the amount of exhumation as well as the timing of its onset. (c) Resulting age versus length plot; shaded area represents mean length \pm standard deviation for samples from different palaeotemperatures (scale on top). Samples from the base of the fossil PAZ produce the low-age peak in the diagram and date the onset of exhumation. Insets show modelled fission track length distributions for rocks originating (from left to right) from below, within and above the PAZ. Modified from van der Beek *et al.* (1996).

Up to 3 km of Karoo sediments were deposited in half-graben bounded by the same faults as those which were active during Late Cenozoic rifting (Morley *et al.*, 1992; Kilembe and Rosendahl, 1992; Mbede, 1993). Karoo rifting also took place along northeast-southwest orientated zones such as the Ruhuhu, Luangwa and Usangu Basins (Wopfner, 1990; Fig. 2), but only some of the northeast trending Karoo basins have been moderately reactivated during the Pleistocene (Delvaux *et al.*, 1992). Unconformably overlying the Karoo Supergroup is the Red Sandstone Group (or "Dinosaur Beds";

Dixey, 1928), deposited during a phase of extension that took place between the Karoo and Late Cenozoic events. The age of this event remains controversial however, with recent estimates ranging from Late Jurassic-Early Cretaceous to Miocene (e.g. Jacobs *et al.*, 1989; Dypvik *et al.*, 1990; Wescott *et al.*, 1991; Damblon *et al.*, 1998).

The latest stage of rifting in the Rukwa-Malawi region commenced at around 8 Ma, as shown by $^{40}\text{Ar}/^{39}\text{Ar}$ dating of rift-related volcanics and field relationships (Ebinger *et al.*, 1989, 1993); the oldest rift-related deposits contain Upper

Miocene palynomorphs and mammalian fossils (Wescott *et al.*, 1991). This phase is still active today, as indicated by historical volcanism and instrumental seismicity (e.g. Delvaux and Hanon, 1993; Jackson and Blenkinsop, 1993; Camelbeeck and Iranga, 1996). The Cenozoic extension direction of basins within the Western Rift is controversial and has been variously inferred as either purely extensional (northeast-southwest; Ebinger *et al.*, 1987; Morley *et al.*, 1992), strike-slip (northwest-southeast; Tiercelin *et al.*, 1988; Wheeler and Karson, 1989; 1994) or initially radial changing to pure extension (Delvaux *et al.*, 1992; Ring *et al.*, 1992). The present-day stress regime from earthquake focal mechanisms appears to be northeast-southwest (Jackson and Blenkinsop, 1993; Camelbeeck and Iranga, 1996).

APATITE FISSION TRACK THERMOCHRONOLOGY

Background

Over the past decade, apatite fission track (AFT) thermochronology has become an extremely valuable technique to constrain the low temperature (< 120°C) thermal histories of exhumed basement blocks (*cf.* Brown *et al.*, 1994 for a review). Tracks are produced continuously over geological time by spontaneous fission of ²³⁸U and the accumulation of fission tracks in minerals such as apatite thus provides a measure of sample age. The tracks are not stable, however, but anneal at strongly temperature-dependent rates. At temperatures between ~60 and 120°C the amount of annealing in apatite increases rapidly towards total; this temperature range has been termed the partial annealing zone (PAZ; Wagner, 1979). The temperature-dependence of annealing rates is now quantitatively understood (Laslett *et al.*, 1987; Green *et al.*, 1989b) and, under tectonically stable conditions, AFT ages and mean track lengths decrease predictably with increasing temperature and hence depth (Fig. 3a). The main control on the decrease of AFT ages and track lengths with depth is exerted by the geothermal gradient; secondary controls are exerted by the duration of tectonically stable conditions and chemical composition, with F rich apatites annealing more quickly than Cl rich apatites (Green *et al.*, 1989a; Crowley *et al.*, 1991).

When a tectonic block cools as a result of denudation, remnants of the characteristic AFT age-depth pattern may be retained,

producing a trend of increasing AFT ages with elevation (Fig. 3b). The base of the exhumed (or "fossil") PAZ, when exposed, will produce a characteristic break in slope in the age-elevation plot, the age of which approximates to the initiation of cooling and denudation (Gleadow and Fitzgerald, 1987). Samples from below the break in slope were exhumed from temperatures $\geq 120^\circ\text{C}$ and contain only tracks formed during and after cooling. In contrast, samples above the break in slope contain two generations of tracks, one from before and one from after the onset of cooling. The actual shape of the age-elevation plot, and the trend of track length distributions with elevation, will depend on the amount and rate of exhumation (Brown *et al.*, 1994).

The dependence of track length distributions (Gleadow *et al.*, 1986) on thermal history can also be used to constrain the amount and timing of rock cooling. A plot of fission track age against mean track length of an exhumed terrain will show a characteristic 'boomerang' shape (Fig. 3c), the length of the peak at young ages corresponding to samples which were exhumed from the base of the PAZ and thus retains only tracks formed after the onset of cooling (e.g. Omar *et al.*, 1989). These samples exhibit narrow, negatively skewed track length distributions with relatively long mean lengths. In contrast, samples which resided within the PAZ before the onset of denudation will typically show wide, bi-modal track length distributions (Fig. 3c). Because the kinetics of annealing in apatite are now quantitatively understood, the observed track length distribution can be used to reconstruct the cooling trajectory (*T-t* path) below 120°C of a sample through inverse modelling (e.g. Lutz and Omar, 1991; Gallagher, 1995).

It should be noted that fission track thermochronology strictly records the cooling of a sample only. Where fission track data show the characteristic relationship to elevation described above, or when additional geological data are available (e.g. the correspondence of cooling intervals with periods of sediment deposition in nearby sedimentary basins or the presence of erosion surfaces of corresponding age), cooling can be interpreted to result from denudation. The amount of denudation can be quantified if the geothermal gradient is known. Inferring uplift from AFT data involves another interpretative step and can only be done if the initial elevation of the region and the degree of isostatic compensation of denudation are known

or inferred (e.g. Brown *et al.*, 1994; van der Beek *et al.*, 1994).

Previous fission track studies in East Africa

Previous AFT studies around the EARS include reconnaissance studies by van den Haute (1984) in Rwanda and Burundi and by Wagner *et al.* (1992) in Kenya, a detailed study of four mountain ranges surrounding the central Kenya Rift (Foster and Gleadow, 1992, 1996) and a regional study in Tanzania (Noble, 1997; Noble *et al.*, 1997). Both van den Haute (1984) and Wagner *et al.* (1992) found that their AFT data indicated slow continuous cooling of basement rocks throughout the last 300-400 Ma. Only samples from very close to the Tanganyika-Kivu and Kenya Rifts showed AFT ages and track length distributions indicative of Tertiary cooling, either through moderate denudation (van den Haute, 1984) or after reheating (Wagner *et al.*, 1992) of the flanks.

Foster and Gleadow (1992, 1996) constructed a composite age-elevation profile from four regions surrounding the central Kenya Rift and were able to distinguish three episodes of rapid denudation during Meso-Cenozoic times: at ≥ 220 , 140-120, and 60-70 Ma. Of these, the Early Tertiary (60-70 Ma) event appears the most important, with up to 2.5 km of denudation recorded; the other two events are associated with ~ 0.5 km of denudation each. Inverse modelling of track length distributions from the eastern flank of the Kenya Rift indicated $\sim 40^\circ\text{C}$ of Miocene-Recent cooling, probably associated with Late Cenozoic rifting. Foster and Gleadow (1993) related the episodes of rapid denudation to intracontinental tectonic phases, correlated to changes in plate motion, which gave rise to block faulting and local uplift. They also showed that the denudation history inferred from their AFT data is inconsistent with classical correlations of regional erosion surfaces, because samples from inferred Mesozoic erosion surfaces remained at depths ≥ 2 km until after 60 Ma.

In Tanzania, Noble *et al.* (1997) found that most of their samples record protracted slow cooling histories throughout the Meso-Cenozoic, interrupted by episodes of faster cooling at around 110 Ma (in eastern Tanzania only) and ~ 65 Ma (throughout eastern and southern Tanzania). They interpret the significance of these accelerated cooling events, similar to Foster and Gleadow (1993), as caused by block faulting during periods of intracontinental tectonics.

APATITE FISSION TRACK DATA FROM THE MALAWI-RUKWA RIFTS

Sampling and procedures

Samples for AFT analysis were collected from both flanks of the Malawi and Rukwa Rifts (Fig. 1). All samples were collected from Ubendian basement rocks; sampled lithologies include granites, ortho- and para-gneisses, amphibolites and anorthosites. In the Livingstone Mountains, a profile (eight samples) spanning an elevation from lake level (400 m) to the summit plateau at 2200 m was collected, as well as a transect (four additional samples) from the top of the escarpment up to 70 km north-northeast of it. In the Kyela region, west of the Malawi Rift, six samples were collected from areas within the rift and up to 50 km west of it, spanning an elevation range from 600 to 2020 m. Two samples were collected from basement underlying Karoo sediments in the Songwe district, in the northwestern sector of the Malawi Rift. Three samples were collected from basement inliers in the Mbeya region, in the intersection between the Malawi, Rukwa and Usangu Basins. AFT data are also reported for nine samples from the Rukwa Rift flanks, which were collected by Mbede *et al.* (1993) from elevations between 910 and 2185 m, close to the eastern and western border faults of the rift. The latter samples were processed by the London Fission Track Research Group (Mbede *et al.*, 1993), while those from the Malawi Rift were processed at the Vrije Universiteit, Amsterdam (van der Beek, 1995). Sample preparation and processing techniques followed the recommendations of Hurford (1990); details can be found in the reports mentioned above.

Results

AFT results are presented in Table 1; their geographical distribution is shown in Fig. 1. All ages are reported as central ages (Galbraith and Laslett, 1993), with a $\pm 1\sigma$ error. AFT ages range from 30 ± 15 to 296 ± 10 Ma, spanning a range in age from the Karoo to Late Cenozoic rifting events. All AFT ages are much younger than the latest Pan-African tectonothermal event. They are interpreted as representing the long-term cooling history of basement rocks resulting from regional denudation. The samples have relatively short mean track lengths (MTL), within the range of 11.4 to 13.2 μm , and broad track length distributions (FTLD) with $\sigma = 1.3$ -2.0 μm (Fig. 4).

Table 1. Fission track analytical data

Sample	Elevation (m)	Number of grains	ρ_s (N_s) ($\times 10^6$ cm $^{-2}$)	ρ_i (N_i) ($\times 10^6$ cm $^{-2}$)	ρ_d (N_d) ($\times 10^6$ cm $^{-2}$)	P(χ^2) (%)	age $\pm 1\sigma$ (Ma)	D (%)	MTL (μ m)	std. (μ m)	No. of tracks
<i>Livingstone Mountains</i>											
DD013	1890	16	3.578 (485)	4.707 (319)	2.551 (13584)	10	217 \pm 20	15	12.6 \pm 0.1	1.3	100
DD298	1840	16	1.880 (973)	2.779 (719)	0.251 (3122)	10	192 \pm 15	13	11.7 \pm 0.2	1.6	80
DD486	1990	20	0.911 (216)	1.054 (125)	2.551 (13584)	90	246 \pm 31	10	12.3 \pm 0.2	1.6	100
DD115a	2200	20	1.627 (1080)	2.136 (709)	2.551 (13584)	5	216 \pm 15	15	12.5 \pm 0.2	1.5	160
DD478	2060	15	1.260 (355)	1.646 (232)	2.511 (13584)	75	214 \pm 22	10			
DD122	1530	15	2.852 (1296)	4.459(1013)	0.251 (3122)	75	178 \pm 14	9	12.2 \pm 0.4	1.5	64
DD483	1340	13	0.345 (78)	1.069 (121)	2.551 (13584)	\ll 1	30 \pm 15	145			
DD482	1110	20	0.110 (102)	0.184 (85)	0.251 (3122)	99	170 \pm 27	5	12.1 \pm 0.4	2.0	28
DD484	905	15	0.905 (914)	3.951(1996)	0.251 (3122)	\ll 1	66 \pm 6	25	11.8 \pm 0.3	2.0	62
DD480	675	16	0.229 (165)	1.304 (470)	0.251 (3122)	75	50 \pm 6	11	11.0 \pm 0.4	1.8	24
DD485a	460	15	0.289 (96)	0.643 (107)	2.551 (13584)	90	128 \pm 20	7	12.1 \pm 0.3	1.7	40
<i>Mbeya region</i>											
DD503	890	15	0.051 (71)	0.430 (302)	0.251 (3122)	5	35 \pm 6	36			
T/92/22b	1280	15	0.180 (55)	0.110 (169)	0.251 (3122)	\ll 1	64 \pm 16	70			
T/92/22a	970	12	0.075 (21)	0.653 (92)	0.251 (3122)	99	33 \pm 8	3			
<i>Western flank (Kyela region)</i>											
DD512	2020	20	1.279 (1034)	2.659(1075)	0.251 (3122)	10	135 \pm 10	14	12.4 \pm 0.2	1.5	100
DD510	1250	12	0.261 (124)	0.391 (39)	0.251 (3122)	75	188 \pm 29	9	12.0 \pm 0.3	1.8	33
DD509	1120	9	0.601 (211)	1.709 (300)	0.251 (3122)	50	100 \pm 12	12			
DD508	1000	20	0.542 (343)	1.131 (358)	0.251 (3122)	50	137 \pm 13	13	11.4 \pm 0.2	1.6	60
DD514a	650	20	0.092 (94)	0.121 (62)	0.251 (3122)	99	214 \pm 37	4			
DD329a	600	18	0.104 (90)	0.159 (69)	0.251 (3122)	99	186 \pm 33	4			
<i>Rukwa Rift (Mbede et al., 1993)</i>											
T/89/25a	1010	20	0.719 (341)	0.622 (295)	1.334 (9506)	60	262 \pm 21		12.4 \pm 0.3	2.3	46
T/89/25b	970	20	0.438 (285)	0.497 (323)	1.339 (9506)	50	202 \pm 16		12.4 \pm 0.3	1.8	46
T/89/26a	1055	20	0.947 (961)	0.929 (943)	1.349 (9506)	\ll 1	239 \pm 11		12.1 \pm 0.2	1.8	100
T/89/26b	985	20	0.456 (265)	0.391 (227)	1.344 (9506)	70	264 \pm 26		12.8 \pm 0.2	1.8	73
T/89/26c	910	20	1.047 (878)	1.002 (840)	1.354 (9506)	65	241 \pm 12		11.7 \pm 0.2	1.7	100
T/89/9d	2185	17	1.219 (289)	1.802 (427)	1.312 (9089)	80	148 \pm 11		13.0 \pm 0.4	1.3	10
T/89/17a	1850	20	1.399 (944)	1.098 (741)	1.312 (9089)	\ll 1	271 \pm 21		11.8 \pm 0.2	1.7	66
T/89/20b	1985	20	2.657 (2762)	1.951(2028)	1.312 (9089)	25	296 \pm 10		12.8 \pm 0.2	2.0	100
T/89/21a	1520	20	2.344 (1017)	3.080(1336)	1.312 (9089)	\ll 1	172 \pm 12		13.2 \pm 02	1.3	43

Notations: ρ_s : spontaneous track density; ρ_i : induced track density (includes 0.5 geometry factor); ρ_d : density of tracks in the glass dosimeter; N_s , N_i , N_d : number of tracks actually counted to determine the reported track densities. All ages are reported as central ages (Galbraith and Laslett, 1993). Employed ζ -factors for the samples processed at the VU Amsterdam (all samples labelled DD and T/92) are 113.6 ± 3.8 for glass dosimeter CN2 ($\rho_s = 2.551 \times 10^6$ cm $^{-2}$) and 11493 ± 522 for NBS963 ($\rho_s = 0.251 \times 10^6$ cm $^{-2}$); the ζ -factor for the samples processed by the London Fission Track Research Group (samples labelled T/89 and EAR797) is 347 ± 5 (glass dosimeter CN5). P(χ^2): Chi-squared probability that the single grain ages represent one population; D: age dispersion. If P(χ^2) < 5 and/or D > 15 the single grain ages represent a multiple age population (cf. Galbraith, 1990; Galbraith and Laslett, 1993).

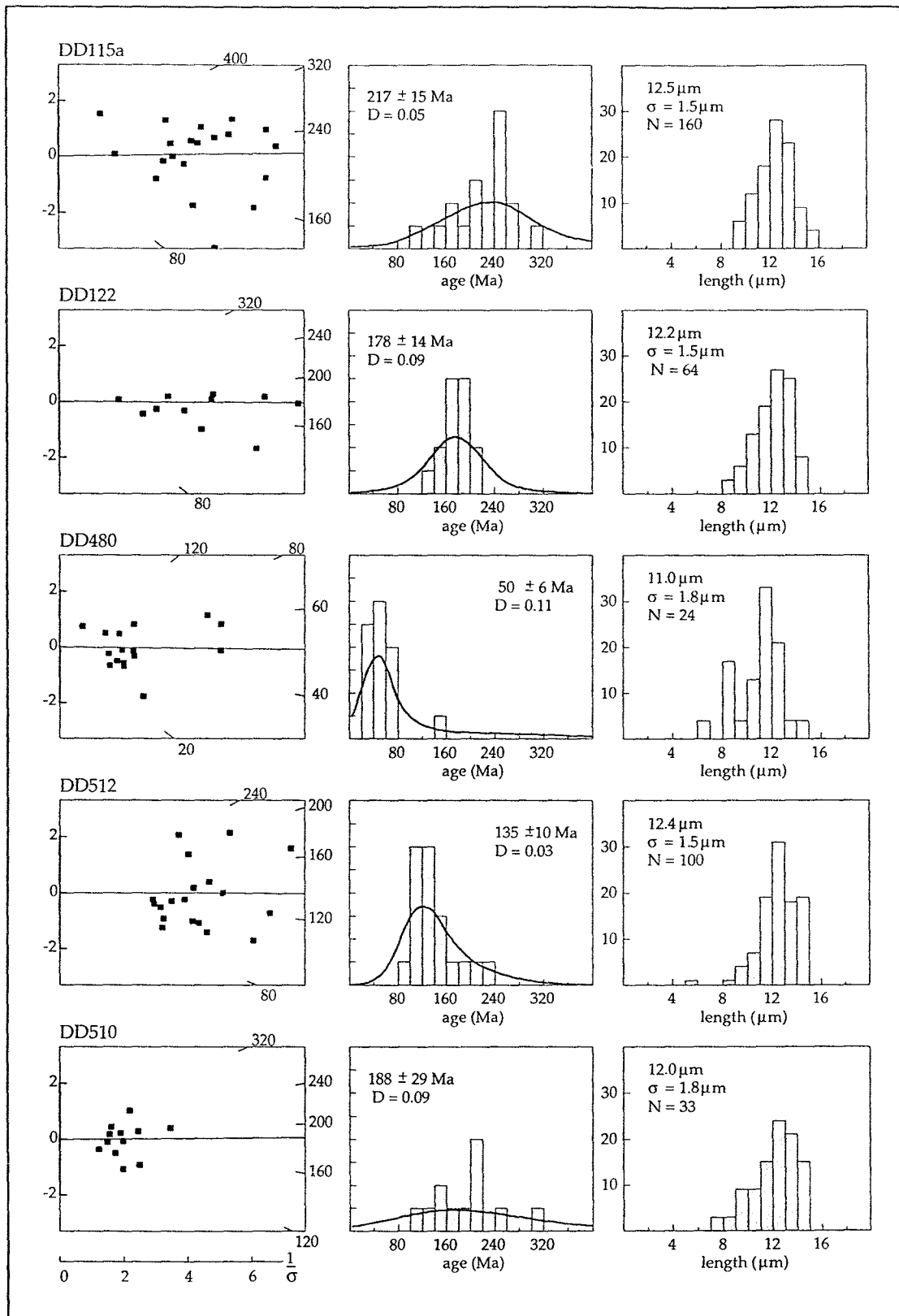


Figure 4. AFT ages and track length distributions for representative samples. Single-grain age distributions are plotted in radial plots (left) and as age histograms and probability curves (centre). Radial plots show the precision of individual track counts on the x-axis and their deviation with respect to the central age on the y-axis (cf. Galbraith, 1990). Histograms of confined track length distributions are shown on the right. Sample DD115a is from the Livingstone Mountains summit; DD122 from the Livingstone Mountains Escarpment at an elevation of ~1500 m; DD480 is from the foot of the Livingstone Mountains Escarpment; DD512 is from the Kyela region just west of the rift; DD510 is from ~50 km west of the Malawi Rift.

Livingstone Mountains

Samples from the Livingstone Mountains show a clear variation of AFT age and MTL with elevation (Fig. 5a). Sample ages from the summit plateau at elevations ≥ 1890 m (DD013, 486, 115a, 478) are concordant between 214 ± 22 and 246 ± 31 Ma. These samples also have very similar track length distributions, with MTL = 12.3 - $12.6 \mu\text{m}$ and $\sigma = 1.3$ - $1.6 \mu\text{m}$. One sample from the summit plateau to the south of the profile (Kalunduru granite), dated by the London Fission Track Research Group (Mbede *et al.*, 1993) has a slightly older but overlapping age of 266 ± 27 Ma. Below 1850 m, AFT ages increase with increasing elevation, from 50 ± 6 Ma at 675 m (DD480) to 192 ± 15 Ma at 1840 m (DD298). MTL for these samples are short, ranging from 11.0 to $12.2 \mu\text{m}$, and FTLD are wide, with $\sigma = 1.5$ - $2.0 \mu\text{m}$. There are two outliers within this general pattern: sample DD483 records an anomalously low AFT age of 30 ± 15 Ma, with an extreme age dispersion (145%); most of the grains in this sample have zero ages, the rest record a spread in ages between 65 and 180 Ma (Fig. 6). Sample DD485 from the foot of the scarp has a much older age (128 ± 20 Ma) than the two samples immediately above it, but does fall on a linear age-elevation trend line ($\sim 0.02 \text{ km Ma}^{-1}$) with the higher ($> 1 \text{ km a.s.l.}$) samples. Of the two intermediate samples, DD480 has a well defined age of 50 ± 6 Ma ($D = 11\%$), whereas the age dispersion of DD484 ($D = 25\%$) indicates multiple age components; most of the grains in this sample have ages between 40-80 Ma, but some are significantly older.

Western flank of the Malawi Rift (Kyela region)

The western flank of the Malawi Rift is topographically less prominent compared to the sharp scarp of the Livingstone Mountains. Samples from the Kyela region show an unusual inverse age-elevation relationship (Fig. 5b). The data do show a clear geographical spread however (Fig. 1). Samples DD329a and DD514a from basement outcrops in and around the Songwe coal mine, still within the Karoo Basin, have AFT ages of 186 ± 33 and 214 ± 37 Ma, respectively. These ages are comparable with those of samples from the summit of the Livingstone Mountains. Both samples from the Songwe mine contained insufficient tracks for FTLD measurements. Immediately to the west of the rift, a group of three samples (DD508, 509, 512) from elevations between 1 and 2 km have younger ages; between 100 ± 12 and

137 ± 13 Ma, with MTL between 11.4 and $12.4 \mu\text{m}$ and $\sigma = 1.5$ - $1.6 \mu\text{m}$. The westernmost sample (DD510) again has an age of 188 ± 29 Ma, with MTL = $12.0 \mu\text{m}$ and $\sigma = 1.8 \mu\text{m}$. This sample resembles those from the Songwe coal mine and from the Livingstone Mountains summit.

Mbeya region

The three samples from the northeasternmost part of the Malawi Rift all have very young AFT ages. Two samples (T92/22a and b) were taken from the northern extension of the Livingstone Mountains, close to the LMBF. T92/22a has an age of 33 ± 8 Ma; this represents a single age population (age dispersion $D = 3\%$); T92/22b, on the other hand, has a large age dispersion ($D = 70\%$) with a central age of 66 ± 16 Ma and single grain ages between 6 and 150 Ma (Fig. 6). The third sample from this region (DD503) was collected from a small basement inlier adjacent to the Mbaka Fault (*cf.* Delvaux and Hanon, 1993; Ebinger *et al.*, 1993); this sample has an age of 35 ± 6 Ma with a dispersion of $D = 36\%$, also suggesting multiple age populations. None of these samples had sufficient tracks for track length measurements. All samples from the Mbeya region were collected close to the Rungwe volcanic centre, one of the main centres of recent volcanic activity in the EARS. It is likely that the volcanics significantly perturbed the geothermal gradient in this area, leading to recent reheating of the samples.

Rukwa Rift

Five samples (T89/25a, b and T89/26a, b, c) from the eastern flank of the Rukwa Rift (the Lupa Plateau) have ages between 202 ± 16 and 264 ± 26 Ma, with MTL between 11.7 and $12.4 \mu\text{m}$ and $\sigma = 1.7$ - $2.3 \mu\text{m}$. These ages and FTLD are comparable to those from the Livingstone Mountains summit plateau. In contrast, two of the samples from the western flank of the Rukwa Rift (the Ufipa Plateau) have the oldest ages in this study (271 ± 21 - 296 ± 10 Ma), whereas the other two have ages that are comparable to samples from the Kyela district: 148 ± 11 and 172 ± 12 Ma. The latter two samples have the highest MTL (13.0 - $13.2 \mu\text{m}$) of all samples in this study, with a relatively narrow FTLD ($\sigma = 1.3 \mu\text{m}$). The nine samples from the Rukwa Rift flanks do not show an obvious age-elevation trend (Mbede *et al.*, 1993; Fig. 5c), probably because all samples from the Lupa Plateau were taken at comparable elevations ($\sim 1 \text{ km a.s.l.}$).

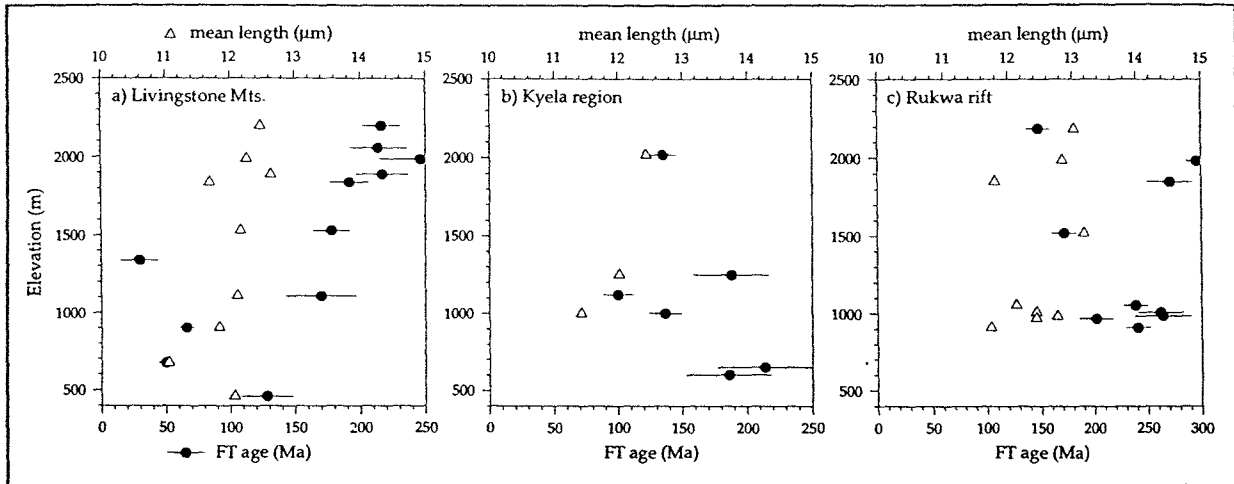


Figure 5. Age-elevation and mean track length-elevation profiles for fission track samples from (a) the Livingstone Mountains to the east of the Malawi Rift; (b) the Kyela profile on the western flank of the Malawi Rift; and (c) the flanks of the Rukwa Rift.

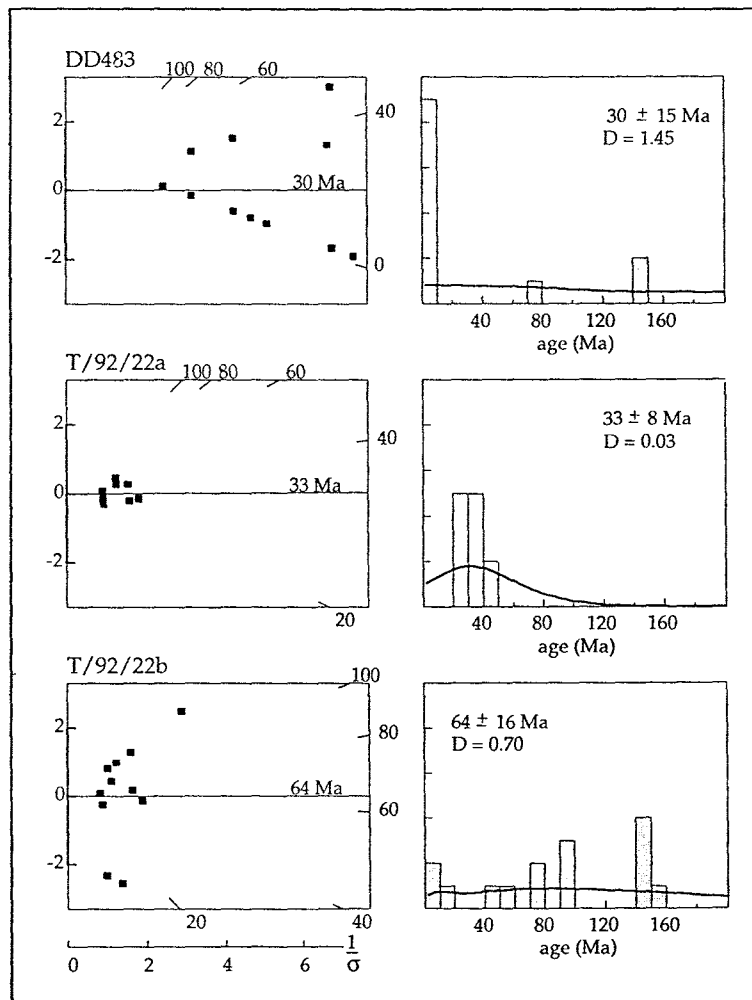


Figure 6. Single grain age distributions for the youngest samples in this study, plotted in radial plots (left) and as age histograms and probability curves (right).

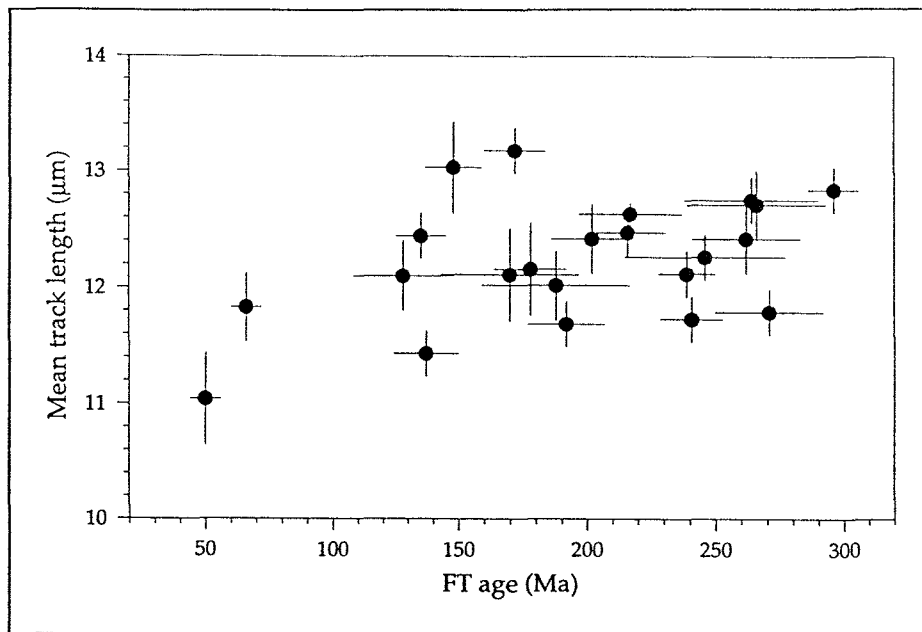


Figure 7. Plot of mean track length against AFT age for samples from this study and from Mbede et al. (1993).

Interpretation: thermotectonic evolution of the Malawi-Rukwa region

The relatively short mean track lengths (MTL) and broad track length distributions (FTLD) of most samples suggest a protracted cooling history spanning the entire Mesozoic and Cenozoic eras (e.g. Gleadow *et al.*, 1986; Green *et al.*, 1989a). The trend of the age-elevation profile from the Livingstone Mountains suggests long-term denudation rates from this region in the order of 20 m Ma^{-1} , assuming that the thermal structure of the Livingstone Mountains block has remained stable throughout this time. However, the track length data indicate that such an interpretation is overly simple.

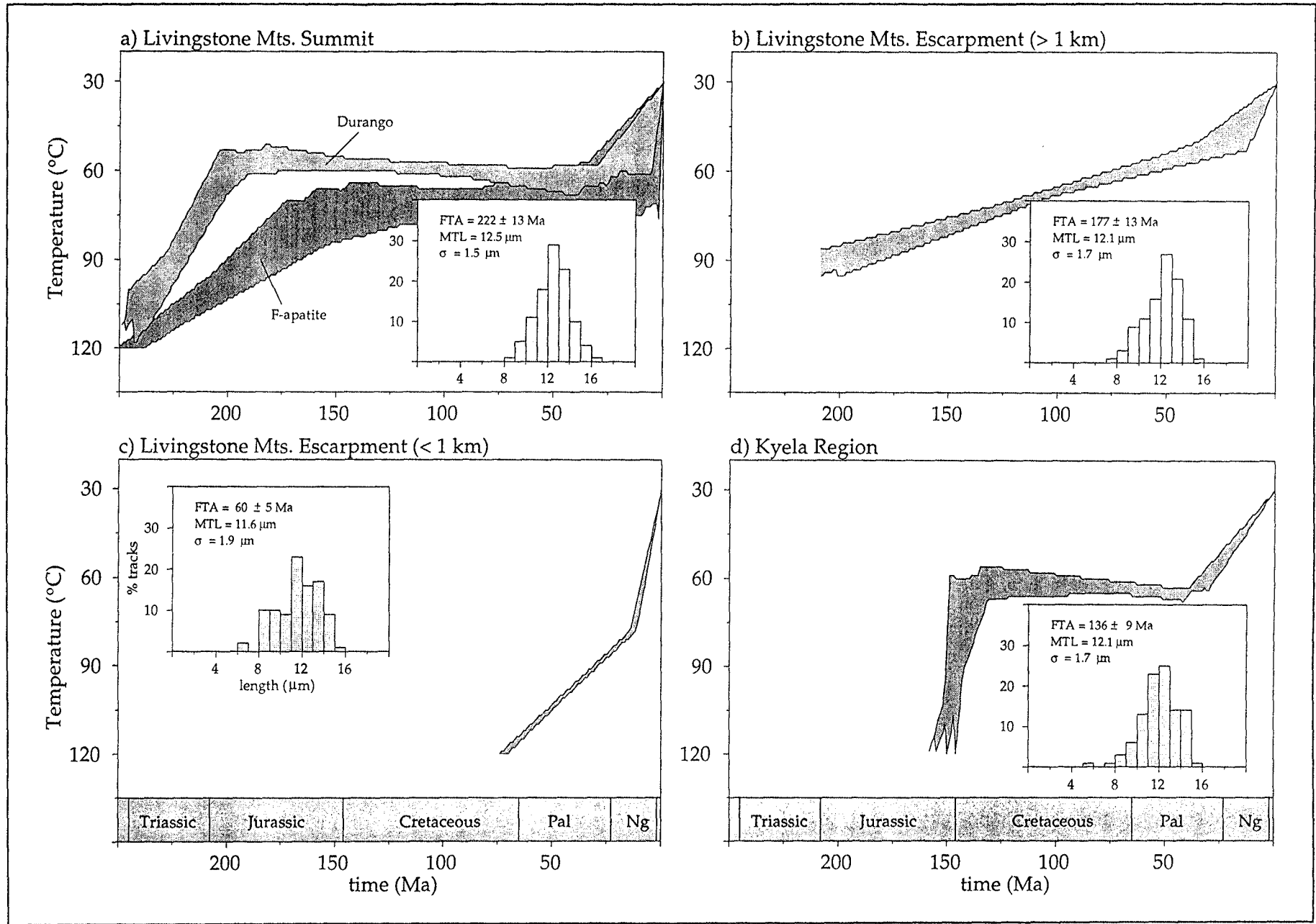
A plot of AFT age versus MTL (Fig. 7) suggests that the long-term thermotectonic history of the region was punctuated by several phases of accelerated cooling. Samples from the summits of the Livingstone Mountains and the Lupa Plateau plot to the right in this diagram, being characterised by ages between ~ 200 - 300 Ma and MTL between ~ 12.2 - $12.8 \mu\text{m}$. FTLD of these

samples are narrower than of most other samples in this study ($\sigma \approx 1.3$ - $1.8 \mu\text{m}$) and are generally uni-modal. These samples record cooling through the PAZ (ie. from $> 120^\circ\text{C}$ to $\sim 60^\circ\text{C}$) at around 200 - 250 Ma .

A peak in MTL (12.4 - $13.2 \mu\text{m}$) is apparent in Fig. 7 around 140 - 170 Ma . Samples with these characteristics derive from the western flanks of the Rukwa and Malawi Rifts. These samples have narrow ($\sigma = 1.3$ - $1.5 \mu\text{m}$) and uni-modal FTLD, suggesting that they cooled relatively rapidly through the PAZ at around $150 \pm 20 \text{ Ma}$.

Finally, samples from the Livingstone Mountains Escarpment form a band of decreasing MTL with decreasing age. The youngest samples in this suite also have the lowest MTL ($< 12.0 \mu\text{m}$) with wide ($\sigma = 1.5$ - $2.0 \mu\text{m}$) negatively skewed or bi-modal FTLD. These samples remained at temperatures $\geq 120^\circ\text{C}$ until Late Mesozoic-Early Cenozoic times (60 - 70 Ma). The abundance of short tracks in these samples indicate that final cooling to surface temperatures took place relatively recently.

Figure 8. Modelled thermal histories for representative samples from the Malawi Rift flanks. Thermal histories within the shaded bands fit the observed AFT ages within 1σ error and pass the Kolmogorov-Smirnov test for track length distribution at the 95% confidence level (cf. van der Beek, 1995). Insets show AFT ages and FTLD used as input for the modelling. (a) Livingstone Mountains summit (combined inversion of samples DD013, DD486 and DD115a, 56 single grain ages and 360 track length measurements in total). The light shaded band labelled "Durango" is for the inversion adopting the Laslett et al. (1987) parameterisation for Durango apatite; the dark band labelled "F-apatite" adopts the Crowley et al. (1991) parameterisation for F apatites (see text for discussion). (b) Livingstone Mountains Escarpment, $> 1 \text{ km a.s.l.}$ (samples DD122 and DD482, total of 35 single grain ages and 92 track length measurements). (c) Base of the Livingstone Mountains Escarpment (samples DD484 and DD480, total of 31 single grain ages and 86 track length measurements). (d) Kyela region (western flank of the Malawi Rift; samples DD508 and DD512, total of 40 single grain ages and 160 track length measurements).



In order to assess the cooling histories of the different subregions within the study area more quantitatively, the thermal histories have been reconstructed from the track length distributions of a number of representative samples, using the inverse modelling approach of van der Beek (1995). The inversion is based on the notion that each track, depending upon its formation during the cooling history of the sample, will record a specific part of this history through a reduction in its length (e.g. Green *et al.*, 1989b). Thus, a given track length distribution can be related quantitatively to a thermal history, using a mathematical description of the annealing process (Lutz and Omar, 1991; Gallagher, 1995). The thermal histories obtained from the inverse modelling of track length distributions are shown in Fig. 8.

Livingstone Mountains

The fact that all samples from the summit plateau of the Livingstone Mountains have concordant AFT ages and similar FTLD is consistent with the interpretation of this plateau as a continuous erosion surface (e.g. Delvaux and Wopfner, 1992). AFT ages and FTLD from the Livingstone Mountains summit plateau are also concordant with those from the Lupa Plateau east of the Rukwa Rift, supporting the interpretation of this surface as a continuous planation level covering a large region. The elevation of the Lupa Plateau is ~1 km lower than that of the Livingstone Mountains summit, suggesting that differential vertical motions have affected the surface after its exhumation.

Figure 8a shows the inferred cooling history for the summit of the Livingstone Mountains, calculated using the combined age and track length data from samples DD013, DD486 and DD115a. The modelling suggests a two-stage cooling history, with cooling from 110–120°C to ~60°C taking place between ~250–200 Ma, followed by a period of relative stability between ~200 and ~40 Ma. Final cooling to surface temperatures took place from ~40 Ma onwards. This cooling history is based on the annealing parameterisation of Laslett *et al.* (1987) for the Durango apatite, with $[Cl]/[Cl + F] \approx 0.2$, whereas most samples from Ubendian basement rocks appear to be nearly pure F apatites (Noble, 1997). In order to test the sensitivity of the inferred cooling history on the chemical composition of the apatites, the inversion was redone using the parameterisation of Crowley *et al.* (1991) for F apatite. This model tends to

predict faster annealing rates compared to the Laslett *et al.* (1987) model at low ($\leq 60^\circ\text{C}$) temperatures, but slower annealing at high ($\geq 90^\circ\text{C}$) temperatures (Corrigan, 1993; van der Beek, 1995). As a result, the two episodes of rapid cooling are less distinct for this model, being smeared out between ~250–150 Ma and ~50–0 Ma, respectively, but they are still clearly distinguishable (Fig. 8a).

The cooling episode between ~200–250 Ma recorded by these samples can be correlated to a widely recognised Late Triassic to Early Jurassic erosion event, which marked the termination of Karoo activity in eastern and southern Africa (Wopfner, 1990, 1993). The AFT data from the summit plateau do not, however, support the inferred Jurassic age of this surface (correlated to the "Gondwana surface" by King, 1963); the scarcity of long ($> 13.5 \mu\text{m}$) tracks in the samples require that they did not cool to surface temperatures during the late Karoo erosional event but only during the Tertiary. A late cooling stage is often inferred from inverse calculations of thermal histories and has been attributed to model artefacts (e.g. Corrigan, 1993). However, because both annealing models employed require late cooling, this study indicates that the late cooling event is real. It is therefore suggested that the maximum exposure age of the Livingstone Mountains summit plateau is Palaeogene (~40 Ma).

The general increase in AFT age with elevation at the Livingstone Mountains Escarpment is consistent with samples from lower elevations having been exhumed from progressively greater depths. There are some irregularities in the pattern however, with sample DD483 having an anomalously young AFT age (30 ± 15 Ma) and DD485a being anomalously old (128 ± 20 Ma). Noble (1997) analysed a suite of samples from an elevation profile spanning from ~500 to 800 m in the Matema region at the northeast corner of the lake, approximately 100 km northwest from the profile studied here. He found similar irregularities, with AFT ages ranging between 20 and 100 Ma and large age dispersions in the majority of his samples. There are three possible explanations for the irregular AFT age pattern at elevations < 1400 m a.s.l. Firstly, the samples may have varying Cl contents, which will affect their annealing characteristics (e.g. Green *et al.*, 1989a; Crowley *et al.*, 1991). At this stage there are no chemical analyses of the samples from this study to investigate this effect. However, inspection of etchpits diameters suggests roughly similar $[F]/$

[CI] ratios for the samples DD480 to DD485a. Samples analysed by Foster and Gleadow (1996) and Noble (1997) from high-grade basement rocks in East Africa also showed little variation in apatite composition, with most grains being nearly pure F apatites. Alternative explanations for the AFT age distribution become apparent if it is considered that the base of the Livingstone Mountains Escarpment coincides with the LMBF, a long-lived crustal-scale shear zone (Wheeler and Karson, 1989; Theunissen *et al.*, 1996). Differential movements of discrete blocks within this fault zone would lead to disruption of the pattern of monotonously increasing AFT ages with elevation (e.g. Fitzgerald, 1994; Foster and Gleadow, 1992, 1996). Samples with young AFT ages would thus define blocks exhumed from structurally deeper levels within the fault zone. Finally, the LMBF has provided a pathway for pervasive fluid flow throughout its history, as indicated by the deposition of a large variety of hydrothermal minerals within the fault zone (e.g. Wheeler and Karson, 1989). Fluid flow activity would have led to leaching, dissolution and re-precipitation of apatite within the LMBF (Noble, 1997). Van der Beek *et al.* (1996) suggested a similar mechanism to account for spurious AFT ages from samples within the Prymorsky Border Fault Zone of the Baikal Rift, a structure very similar to the LMBF. The abundance of zero grain ages in sample DD483 suggests that fluid flow through the fault zone is still active today, as is also indicated by active hydrothermal centres and Quaternary travertine deposits in the Mbeya region, both clearly associated with active faults (Harkin, 1960; Delvaux and Hanon, 1993).

Thermal histories from inverse calculations for samples from the Livingstone Mountains Escarpment are depicted in Fig. 8b (for samples DD122 and DD482, between 1-1.5 km a.s.l.) and 8c (for samples DD484 and DD480, at < 1 km a.s.l.). The modelling suggests that the lowermost samples remained at temperatures $\geq 120^{\circ}\text{C}$ until $\sim 60\text{-}70$ Ma (Late Cretaceous-Palaeogene) and only cooled from $\sim 80^{\circ}\text{C}$ down to surface temperatures in the last ~ 20 Ma. These samples suggest that a significant amount of denudation of the Livingstone Mountains Escarpment has taken place during the Cenozoic, more than half of which took place during Late Cenozoic rifting.

Kyela region

Samples from the basement in and around the Songwe coal mine have ages similar to those

from the summit plateau of the Livingstone Mountains. Although there is no supporting track length data, it is suggested that these samples have experienced a similar cooling history. Karoo deposition took place between Late Carboniferous and Triassic times in Tanzania (e.g. Wopfner, 1990); in the Songwe region only the lower part of the Karoo sediments have been preserved, the youngest unit having a probable mid-Permian age (Semkiwa, 1992). The AFT data from this study indicate that the samples reached maximum temperatures of $\geq 120^{\circ}\text{C}$ before ~ 240 Ma, i.e. shortly after deposition. Vitrinite reflectance ($R_o = 0.5\text{-}1.0$; Kreuser *et al.*, 1988) and Rock-Eval ($T_{max} = 400\text{-}450^{\circ}\text{C}$; Dypvik *et al.*, 1990) data for Karoo coals from southern Tanzania are consistent with this palaeo-temperature estimate. A minimum overburden equivalent to a $\sim 50\text{-}60^{\circ}\text{C}$ temperature difference (the PAZ) was removed during Late Triassic-Early Jurassic denudation. For a geothermal gradient of $25\text{-}30^{\circ}\text{C km}^{-1}$ within the Karoo basins (determined from vitrinite reflectance data by Kreuser *et al.*, 1988) this corresponds to 2.0 ± 0.4 km of removed section.

Samples immediately to the west of the rift (DD512, DD508) record a Late Jurassic - Early Cretaceous cooling event around ~ 150 Ma (Fig. 8d), in addition to Cenozoic (≤ 40 Ma) cooling. Late Jurassic AFT ages are also encountered on the western flank of the Rukwa Rift. Sample DD508 from an elevation of around 1000 m a.s.l. has shorter MTL than sample DD512 from an elevation of above 2000 m (11.4 versus 12.4 μm). Modelling suggests that the lower sample has remained $20\text{-}30^{\circ}\text{C}$ warmer than the topographically higher one from Late Jurassic to Palaeogene times.

The fact that Late Jurassic-Early Cretaceous cooling is only recorded in the western flanks of both rifts suggests that this event was caused by more local denudation, possibly related to block faulting around that time. Seismic data from the Rukwa Rift indicate that the eastern (Lupa) and western (Ufipa) border faults of the rift were active intermittently during its evolution (e.g. Morley *et al.*, 1992; Kilembe and Rosendahl, 1992; Mbede, 1993). Within the Malawi Rift Basin, the possibly Upper Jurassic-Cretaceous Red Sandstone Group ("Dinosaur beds") crops out unconformably on top of Karoo sediments, suggesting renewed rifting and sediment accumulation during that time. Sediment provenance for the Red Sandstones appears to be mainly from the west (Dypvik *et*

al., 1990), consistent with contemporaneous denudation of the western flank. The dating of the Red Sandstones in the Rukwa and Malawi Rifts is, however, controversial (Dambon *et al.*, 1998) and their deposition could also be related to the inferred widespread Cenozoic denudation that is suggested by the modelling.

Regional correlations

The data of this study indicate that the flanks of the Malawi and Rukwa Rifts have experienced accelerated regional cooling (and, by inference, denudation) during Triassic-Early Jurassic (~250-200 Ma), Late Jurassic-Early Cretaceous (~150 Ma) and Tertiary (<40-50 Ma) times. Samples from the base of the Livingstone Mountains Escarpment indicate that more than half of the Cenozoic cooling may have taken place from mid-Miocene (~20 Ma) onwards. Of these cooling events, the Triassic-Early Jurassic and Cenozoic events appear to be most widespread, being recorded by practically all samples. The Late Jurassic-Early Cretaceous event is only recorded by samples from the western flanks of the Malawi and Rukwa Rifts, whereas post-Miocene cooling can only unambiguously be demonstrated from the base of the Malawi footwall flank.

The Triassic-Early Jurassic cooling phase marks the end of the Karoo sedimentary regime and is widely recognised as a major erosional event (e.g. Wopfner, 1993). As denudation during this phase appears to have affected both the Karoo basins and their flanks equivalently, there may have been very little topography left at the end of Karoo times and the erosional episode must have been triggered externally. The Late Jurassic-Early Cretaceous phase is possibly coeval with deposition of the Red Sandstone Group, although the latter may also be correlated with renewed Tertiary cooling. There is thus a close correlation between phases of denudation of the rift flanks and the onset or termination of rifting events, as recorded by the different sedimentary units within the Malawi-Rukwa Rifts.

Brown *et al.* (1990) reported a widespread phase of denudation around 140 ± 10 Ma in southern Africa, whereas Foster and Gleadow (1993) report denudation events at around 220 Ma, 140-120 Ma and 60-70 Ma from central Kenya. The results of this study appear roughly consistent with these previous studies, suggesting that the inferred phases of denudation are of (sub)continental significance. The largest difference in timing appears for the Late Jurassic-Early Cretaceous phase, but this is the least

constrained from the samples of this study. Foster and Gleadow (1993) suggested that such regional phases of denudation can be correlated to periods of plate tectonic reorganisation and intracontinental deformation. For instance, Triassic-Early Jurassic denudation is coeval with the onset of rifting between East Africa and Madagascar (e.g. Wopfner, 1993); the Late Jurassic-Early Cretaceous is the time of initial rifting in the South Atlantic, and the earliest Tertiary event can be correlated with a major plate reorganisation in the Indian Ocean (e.g. Foster and Gleadow, 1993; Janssen *et al.*, 1995). These changes in plate motion appear to be correlated with basin reactivation throughout the African continent (Bosworth, 1992; Janssen *et al.*, 1995).

UPLIFT AND EROSION HISTORY OF THE MALAWI-RUKWA RIFT FLANKS

The morphology of the high level plateaus and uplands flanking the Western Rift system in East Africa have been variably explained as either essentially relict features, initiated by Karoo tectonics and only influenced by erosional processes since then (e.g. Dixey, 1947) or, in contrast, as being a direct result of tectonic uplift during Late Tertiary rifting (e.g. Ebinger *et al.*, 1991, 1993). This study indicates that the rift flanks record a protracted denudation history, with subsequent erosional phases correlated to the different rifting events within the Malawi-Rukwa Rift Zone. This section will discuss attempts to quantify the amounts of denudation that have taken place on the flanks during the different erosional episodes. Subsequent attempts to constrain the relative roles of uplift and erosion in creating the present-day morphology of the flanks through numerical modelling of rifting and flank uplift will be discussed.

Estimates of denudation

Cooling of the upper crust can, in general, be caused either by a reduction in the geothermal gradient or by denudation. In order to constrain the amount of denudation that has occurred, some bounds need to be placed on the geothermal gradient. Mbede (1993) calculated a present-day geothermal gradient of $\sim 40^\circ\text{C km}^{-1}$ for the Rukwa Rift from well-log data within the basin. This intra-basinal thermal gradient cannot be directly extrapolated to the flanking regions, however. A regional study by Nyblade *et al.* (1990) indicates that heat flow within the Pan-

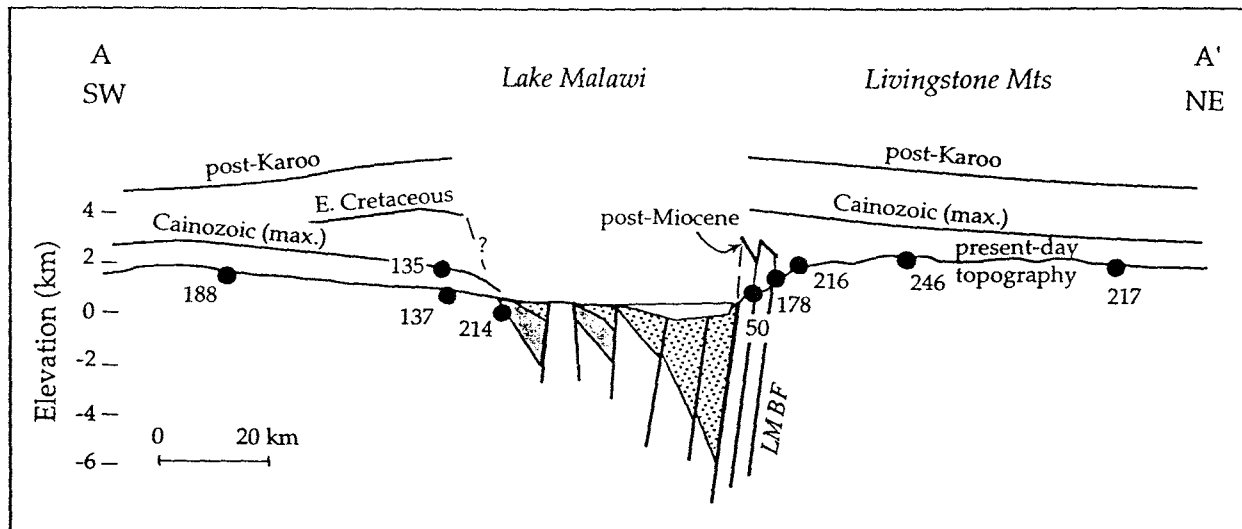


Figure 9. Simplified structural and topographic profile across the northern Malawi Rift (after Ebinger *et al.*, 1993) showing the distribution of representative AFT ages (black dots with numbers) and the reconstructed regional distribution of denudation across the section for the different erosional phases recognised. Note that these "palaeolandsurfaces" do not represent palaeotopographic elevations because they are not isostatically balanced (e.g. van der Beek *et al.*, 1994). The structure of the northern Malawi Rift is from the project PROBE seismic line 804 (e.g. Rosendahl *et al.*, 1992). coarse stippling indicates Late Cenozoic rift deposits; grey shading: Karoo sediments; LMBF: Livingstone Mountains Border Fault.

African mobile belts (including the Karoo and recent rifts) is $\sim 60\text{--}80 \text{ mW m}^{-2}$, whereas the cratons record a much lower heat flow of $\sim 35 \text{ mW m}^{-2}$. For a thermal conductivity of crystalline upper crustal rocks of $\sim 2.5 \text{ W m}^{-1} \text{ K}^{-1}$, these estimates suggest that $25\text{--}30^\circ\text{C km}^{-1}$ is a reasonable value for the present-day geothermal gradient in the Malawi-Rukwa region.

Assuming a surface temperature of $25\text{--}30^\circ\text{C}$, the widespread Cenozoic cooling from $\sim 60^\circ\text{C}$ represents 1.0–1.4 km of regional denudation. Because of the possible artefacts in the annealing models discussed previously, this amount of cooling and denudation must be considered a maximum value. Samples from the foot of the Livingstone Mountains Escarpment record cooling from $\geq 120^\circ\text{C}$ during Tertiary times, which would correspond to 2.7–3.8 km of denudation. Of this amount, $2.2 \pm 0.4 \text{ km}$ (corresponding to cooling from $\sim 80^\circ\text{C}$ down to surface temperatures) appears to have taken place since the Miocene (i.e. post-20 Ma), and probably contemporaneously with the present rifting activity. The summit of the Livingstone Mountains lies at an elevation of 1.5–2 km above the lake level. This elevation difference suggests that Cenozoic uplift and isostatic rebound of the lake shore was greater than that of the Livingstone Mountains summit, 10–20 km away from the rift (Fig. 9).

Constraining the amount of denudation related to the earlier cooling events is more difficult

because there is no direct measure of palaeoheat flow. However, a vitrinite reflectance study by Kreuser *et al.* (1988) suggests that the geothermal gradient through the Karoo basins of southern Tanzania at the time of maximum burial (i.e. $\sim 250 \text{ Ma}$) was around $25\text{--}30^\circ\text{C km}^{-1}$, similar to the present-day gradient. If it is assumed that regional heat flow remained stable during Meso-Cenozoic times, then the $50\text{--}60^\circ\text{C}$ cooling recorded by samples from the western flanks of the Malawi and Rukwa Rifts during the Late Jurassic–Early Cretaceous correspond to $2.0 \pm 0.4 \text{ km}$ of local denudation. The regional denudation event at the end of the Karoo depositional episode would have removed a similar amount of overburden from the entire region (Fig. 9).

The total post-Karoo denudation of the region thus varies between $3.2 \pm 0.6 \text{ km}$ for the summit plateau of the Livingstone Mountains to $5.3 \pm 0.7 \text{ km}$ for the lake shore in front of the Livingstone Mountains Escarpment. Of the three denudation episodes recorded, the late Karoo phase appears to be the most important, removing $\sim 2 \text{ km}$ of material from the entire region. The Late Jurassic–Early Cretaceous event caused similar amounts of denudation, but only on the western flanks of the rifts, whereas Cenozoic denudation was probably $\leq 1 \text{ km}$, except at the Livingstone Mountains Escarpment, where it may have reached $\sim 3 \text{ km}$.

Table 2. Best-fit parameters employed in thermomechanical modelling of extension and rift flank uplift

parameter	symbol	value for the Malawi Rift (van der Beek, 1995)	value for the Rukwa Rift (Mbede, 1993)
crustal thickness (km)	c	40	40
lithospheric thickness (km)	L	150	150
onset of rifting (Ma)	t	8	300 (Karoo) 8 (Cenozoic)
equivalent elastic thickness (km)	T_e	30	28
detachment depth (km)	z_d	30	40
crustal density (kg m^{-3})	ρ_c	2800	
mantle density (kg m^{-3})	ρ_m	3300	
sediment density (kg m^{-3})	ρ_s	2200	2200
extension on fault (km)	e	7.2 (LMBF)	4.0 (Lupa, Karoo) 6.0 (Lupa, Cenozoic) 5.0 (Ufipa, Cenozoic)

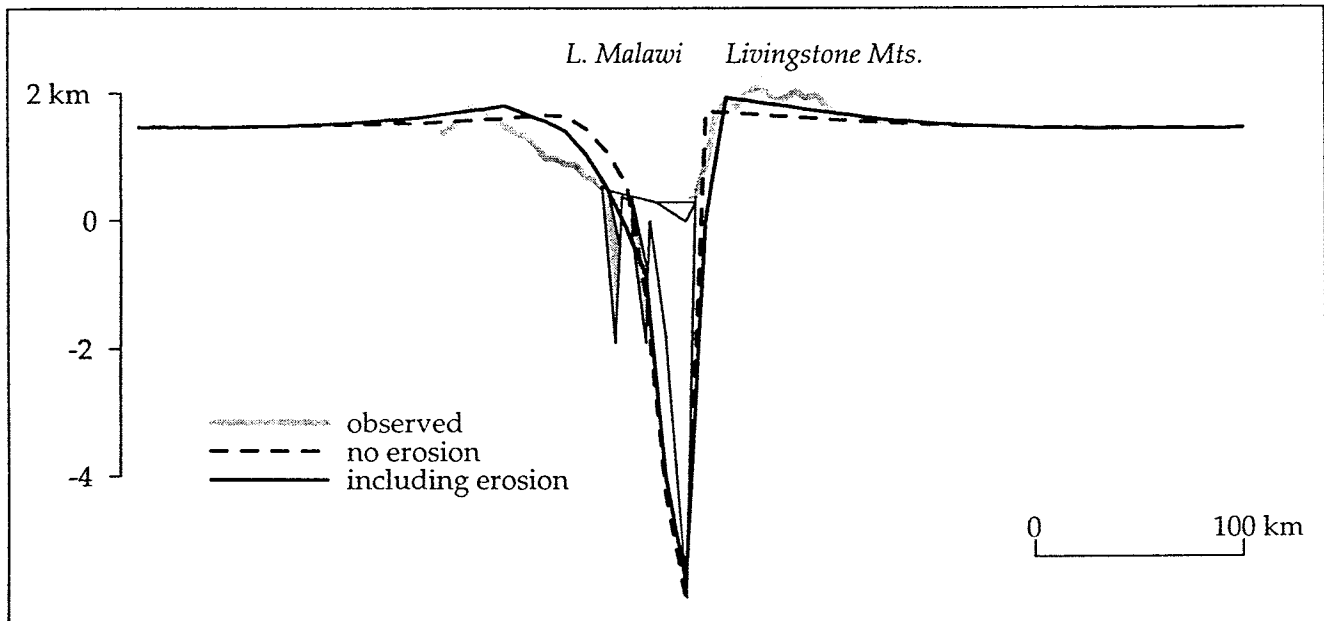


Figure 10. Predicted basin geometry and flank topography for a profile across the northern Malawi Rift, adopting a detachment depth of 30 km, 7.2 km extension on the Livingstone Mountains Border Fault and $T_e = 30$ km, both with and without Cenozoic erosion (amount of erosion as in Fig. 9). The thick grey line indicates the observed topography, light grey shading is the observed Cenozoic basin fill; dark shading: Karoo sediments.

Modelling Cenozoic rift flank uplift and erosion

In order to quantitatively assess the roles of tectonic uplift, erosion and isostatic rebound in controlling topography around the Malawi and Rukwa Rifts, numerical models for continental extension and rift flank uplift have been used. Flank uplift along continental rifts such as the Western Rift of East Africa is best explained as a result of the flexural isostatic response of the

lithosphere to extensional unloading during rifting (e.g. Weissel and Karner, 1989; Ebinger *et al.*, 1991, 1993; van der Beek *et al.*, 1994; Upcott *et al.*, 1996).

A profile which runs across the northern termination of Lake Malawi has been modelled using a thermomechanical model developed by ter Voorde and Cloetingh (1996). In this model, crustal extension is accommodated by slip at a

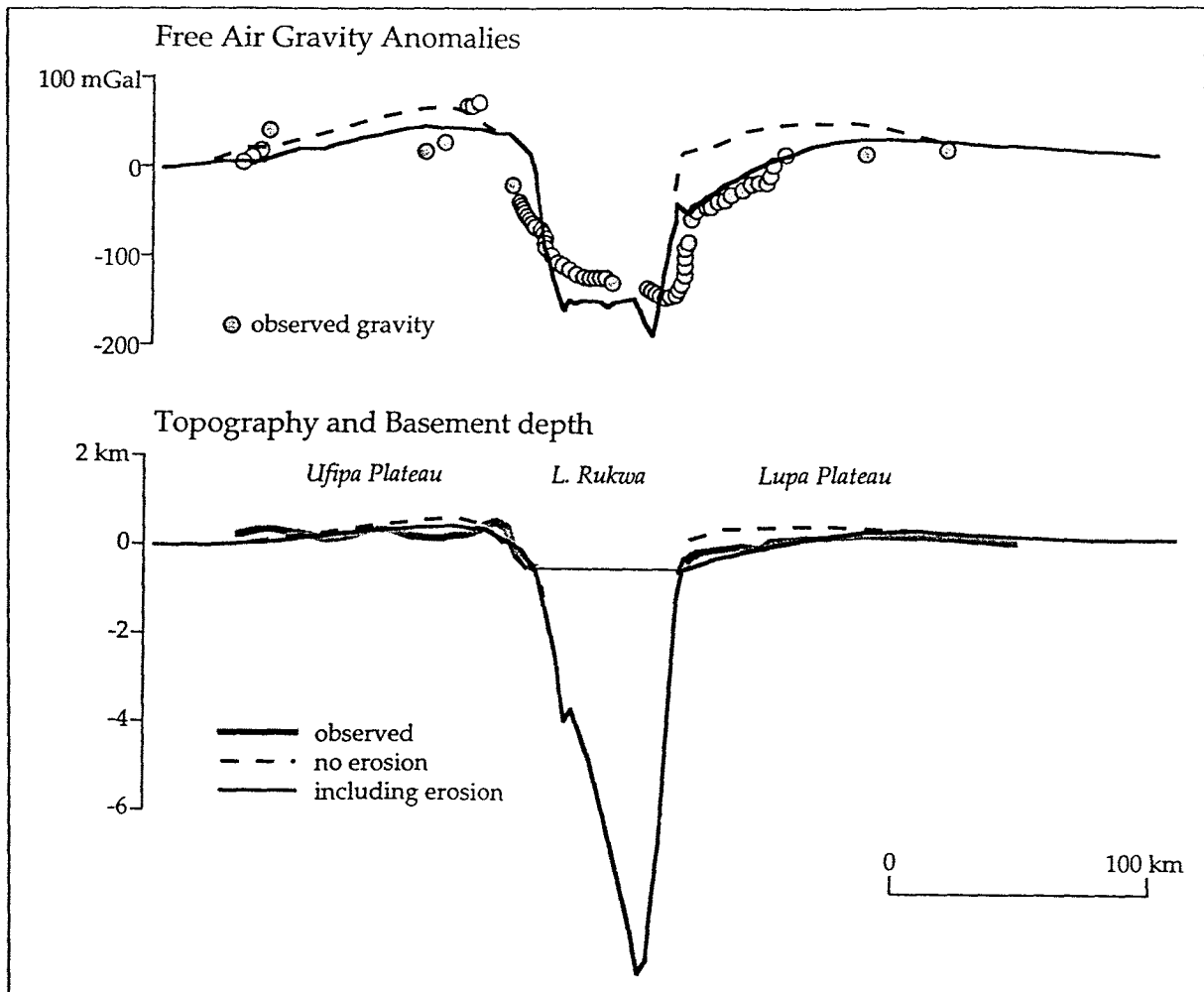


Figure 11. (lower panel) Predicted basin geometry and flank topography for a profile across the central Rukwa Rift, adopting a detachment depth of 40 km, 4 km extension on the Lupa Fault during Karoo rifting and 6 km during Cenozoic rifting, 5 km extension on the Ufipa Fault during Cenozoic rifting, and $T_e = 28$ km, both with and without erosion (after Mbede, 1993). The model is fitted to the observed basement geometry in seismic line TVZ07 (Morley et al., 1992; Kilembe and Rosendahl, 1992; Mbede, 1993). (upper panel) Predicted Free Air gravity anomaly profile, with and without erosion. Note particularly the negative Free Air anomalies over the eastern flank, which provide strong evidence for erosion of the flank.

finite rate along one or more crustal normal faults, and is counterbalanced by distributed pure-shear thinning and extension below the depth at which the fault soles out (the detachment depth z_d). A similar profile was modelled by Ebinger *et al.* (1991, 1993) using the instantaneous extension model of Weissel and Karner (1989); these previous analyses did not take erosion of the rift flanks into account.

The predicted rifting kinematics and isostatic rebound are mainly controlled by three parameters: the shape of the fault, the amount of extension, and the flexural rigidity (or equivalent elastic thickness T_e) of the lithosphere. The border faults of the Malawi and Rukwa Rifts appear to sole out in the middle to lower crust, at a depth of 20–30 km (e.g. Jackson and

Blenkinshop, 1993; Camelbeeck and Iranga, 1996). The amount of extension and T_e of the lithosphere was determined by fitting the basement depth beneath the basin, as observed on seismic reflection profiles, and the elevation of the rift flanks (van der Beek, 1995). Best-fit modelling parameters are given in Table 2. It is assumed that, prior to Late Cenozoic extension, the region was flat and at an elevation of 1.5 km a.s.l., the present-day elevation of most of the Tanzanian Craton.

The modelling results, presented in Fig. 10, suggest that Cenozoic erosion has been an important factor in modifying flank topography. For a detachment depth of 30 km and $T_e = 30$ km, 7.2 km of extension on the LMBF is required to fit the observed basement depth. A model

that does not take erosion of the rift flanks into account does not predict sufficient topography for the footwall flank but over estimates the elevation at the hanging wall side of the rift. If erosion of the flanks is incorporated, the additional isostatic rebound provides a much better fit to the observed elevation of the Livingstone Mountains, whereas the elevation of the western hanging wall flank is lowered. The amounts of Cenozoic erosion incorporated in the modelling are those derived from the FT data and depicted in Fig. 9. This result is consistent with structural studies of the northern Malawi Basin (Ebinger *et al.*, 1993), which indicate that several hundreds of metres of sediment have been eroded from the hanging wall side of the basin since the onset of rifting, the eroded material being redeposited in the depocentre close to the LMBF.

Mbede (1993) used a broadly similar numerical model (Weissel and Karner, 1989; Ebinger *et al.*, 1991) to predict the present-day topography surrounding the Rukwa Rift (Fig. 11). She adopted a two-stage rifting model to predict the basin evolution from the Karoo to recent times, firstly modelling the basement subsidence and flank uplift due to Karoo rifting, then removing the amount of material eroded since Karoo times (e.g. Fig. 9) and calculating the isostatic response, and finally imposing Cenozoic extension. Again, the fit to the observed topography becomes much better when the amount of denudation that is recorded by the AFT data is incorporated in the modelling. Mbede (1993) also used the model to predict Free Air gravity anomalies over the basin, in order to have a separate control on amounts of denudation. The Free Air anomaly is normally more sensitive to changes in crustal thickness due to denudation than topography (*cf.* Ebinger *et al.*, 1991). A comparison of observed and predicted Free Air anomaly profiles (Fig. 11) provides independent evidence for considerable amounts of denudation since Karoo rifting, especially on the eastern (Lupa Plateau) flank of the rift.

CONCLUSIONS

The AFT data from the flanks of the Malawi and Rukwa Rifts record a protracted cooling history with three distinct phases of accelerated cooling and denudation that are related to the different rifting events in the region. Both rifting and denudation appear to be ultimately controlled by continental-scale tectonic events related to changes in plate motions.

The oldest denudation event recorded by the AFT data, at around 250-200 Ma, can be ascribed to late Karoo erosion that affected the entire area. Samples from the Livingstone Mountains summit and those from the eastern flank of the Rukwa Rift define a similar structural level or erosion surface. This surface has traditionally been correlated to the Jurassic "Gondwana surface" of eastern and southern Africa, but the AFT data indicate that final exposure of this surface did not take place before the Palaeogene (~40 Ma).

Samples from the western flanks of the Malawi and Rukwa Rifts record a Late Jurassic-Early Cretaceous (~150 Ma) phase of denudation, possibly related to renewed rifting and the deposition of the Red Sandstone Group. Finally, thermal history reconstructions from inverse modelling of track length distributions suggest that most samples record ~35°C cooling during the Cenozoic. Samples from the base of the Livingstone Escarpment were exhumed from temperatures $\geq 120^\circ\text{C}$ during Cenozoic times, with more than half the denudation taking place since 20 Ma. Estimated amounts of denudation for the late Karoo and Late Jurassic-Early Cretaceous events are 2.0 ± 0.4 km each, whereas Cenozoic denudation probably amounted to $\leq 1.2 \pm 0.2$ km.

Modelling of Cenozoic extension and rift flank uplift indicates that rift related erosion of the flanks has modified the observed topography. The high elevation of the Livingstone Mountains away from the Malawi Rift Zone appears to be caused by regional isostatic response to erosion of the escarpment, whereas the elevation of the hanging wall flank may have been lowered significantly by erosion. Topographic and gravity data from the Rukwa Rift suggest that especially the eastern flank (Lupa Plateau) of that rift has been severely modified by erosion.

ACKNOWLEDGMENTS

This research formed part of the Ph. D. studies of P. van der Beek at the Vrije Universiteit Amsterdam, and E. Mbede at the Technische Universität Berlin. Fieldwork was carried out as part of a UNESCO sponsored geotraverse within the framework of the CASIMIR (Comparative Analysis of Sedimentary Infill Mechanisms in Rifts) project, funded by the Belgian government. The Tanzania Commission for Science and Technology (COSTECH), the University of Dar es Salaam and Madini office provided logistical support. Thanks are due to R. Kajara and J.

Sarota of Madini Dodoma for assistance during sample collection. The London Fission Track Research Group provided AFT dating facilities for the samples from the Rukwa Rift. The other samples were processed at the Vrije Universiteit Amsterdam, with assistance from Lodewijk IJst and Tineke Vogels. The authors thank Wayne Noble for stimulating discussions on the interpretation of AFT data from Tanzania and for providing preprints of parts of his thesis. The manuscript was substantially improved by the comments of C. Ebinger, H. Wopfner and an anonymous reviewer. Netherlands Research School of Sedimentary Geology Publication no 271197. This is a contribution to IGCP400 project "Geodynamics of Continental Rifting".

REFERENCES

- Bosworth, W. 1985. Geometry of propagating continental rifts. *Nature* **316**, 625-627.
- Bosworth, W. 1992. Mesozoic and early Tertiary rift tectonics in East Africa. *Tectonophysics* **209**, 115-137.
- Brown, R. W., Rust, D. J., Summerfield, M. A., Gleadow, A. J. W. and de Wit, M. C. J. 1990. An Early Cretaceous phase of accelerated erosion on the south-western margin of Africa: Evidence from apatite fission track analysis and the offshore sedimentary record. *Nuclear Tracks Radiation Measurements* **17**, 339-350.
- Brown, R. W., Summerfield, M. A. and Gleadow, A. J. W. 1994. Apatite fission-track analysis: Its potential for the estimation of denudation rates and implications for models of long-term landscape development. In: *Process Models and Theoretical Geomorphology* (Edited by Kirkby, M. J.) pp24-53. Wiley, New York.
- Camelbeeck, T. and Iranga, M. D. 1996. Deep crustal earthquakes and active faults along the Rukwa trough, Eastern Africa. *Geophysical Journal International* **124**, 612-630.
- Chorowicz, J. 1990. Dynamics of different basin types in the East African rift. *Journal African Earth Sciences* **10**, 271-282.
- Corrigan, J. 1993. Apatite fission-track analysis of Oligocene strata in South Texas, U.S.A.: Testing annealing models. *Chemical Geology (Isotope Geoscience Section)* **104**, 227-249.
- Crowley, K. D., Cameron, M. and Schaefer, R. L. 1991. Experimental studies of annealing of etched fission tracks in fluorapatite. *Geochimica Cosmochimica Acta* **55**, 1449-1465.
- Daly, M. C., Chorowicz, J. and Fairhead, J. D. 1989. Rift basin evolution in Africa: the influence of reactivated steep basement shear zones. In: *Inversion Tectonics* (Edited by Cooper, M. A. and Williams, G. D.) *Geological Society Special Publication* **44**, 309-334.
- Damblon, F., Gerienne, Ph., d'Outrelepoint, H., Delvaux, D., Beekman, H. and Back, S. 1998. Identification of a fossil wood specimen in the Red Sandstone Group of southwestern Tanzania: stratigraphical and tectonic implications. In: *Tectonics, sedimentation and volcanism in the East African Rift System* (Edited by Delvaux, D. and Khan, M. A.) *Journal African Earth Sciences* **26**, 387-396.
- Delvaux, D. and Hanon, M. 1993. Neotectonics of the Mbeya area, SW Tanzania. *Rapport Annuel 1991-1992*, pp87-97. Département de Géologie et Minéralogie, Musée Royal de l'Afrique Centrale, Tervuren, Belgium.
- Delvaux, D. and Wopfner, H. 1992. Some observations on the geomorphology and recent rift movements in the Livingstone Mountains, SW Tanzania. *UNESCO, Geology Economic Development Newsletter* **9**, 171-173.
- Delvaux, D., Levi, K., Kajara, R. and Sarota, J. 1992. Cenozoic paleostress and kinematic evolution of the Rukwa - North Malawi rift valley (East African rift system). *Bulletin Centres Recherches Exploration Production Elf-Aquitaine* **16**, 383-406.
- Dixey, F. 1928. The Dinosaur beds of Lake Nyasa. *Transactions Geological Society South Africa* **16**, 55-66.
- Dixey, F. 1937. The early Cretaceous and Miocene peneplains of Nyasaland and their bearing on the age and development of the Rift Valley. *Geological Magazine* **74**, 49-82.
- Dixey, F. 1947. Erosion and tectonics in the East African rift system. *Quarterly Journal Geological Society London* **102**, 339-388.
- Dypvik, H., Nesteby, H., Ruden, F., Aagaard, P., Johansson, T., Msindai, J. and Massay, C. 1990. Upper Paleozoic and Mesozoic sedimentation in the Rukwa-Tukuyu Region, Tanzania. *Journal African Earth Sciences* **11**, 437-456.
- Ebinger, C. J. 1989. Tectonic development of the western branch of the East African rift system *Geological Society America Bulletin* **101**, 885-903.
- Ebinger, C. J., Rosendahl, B. R. and Reynolds, D. J. 1987. Tectonic model of the Malawi rift, Africa. *Tectonophysics* **141**, 215-235.
- Ebinger, C. J., Deino, A. L., Drake, R. E. and Tesha, A. L. 1989. Chronology of volcanism and rift basin propagation: Rungwe volcanic province, East Africa. *Journal Geophysical Research* **94**, 15,783-15,803.
- Ebinger, C. J., Karner, G. D. and Weissel, J. K. 1991. Mechanical strength of extended continental lithosphere: constraints from the Western rift system, Africa. *Tectonics* **10**, 1239-1256.
- Ebinger, C. J., Deino, A. L., Tesha, A. L., Becker, T. and Ring, U. 1993. Tectonic controls on rift basin morphology: Evolution of the Northern Malawi (Nyasa) Rift. *Journal Geophysical Research* **98**, 17,821-17,836.
- Fitzgerald, P. G. 1994. Thermochronologic constraints on post-Paleozoic tectonic evolution of the central Transantarctic Mountains, Antarctica. *Tectonics* **13**, 818-836.
- Foster, D. A. and Gleadow, A. J. W. 1992. The morphotectonic evolution of rift-margin mountains in central Kenya: Constraints from apatite fission-track thermochronology. *Earth Planetary Science Letters* **113**, 157-171.
- Foster, D. A. and Gleadow, A. J. W. 1993. Episodic denudation in East Africa: A legacy of intracontinental tectonism. *Geophysical Research Letters* **20**, 2395-2398.
- Foster, D. A. and Gleadow, A. J. W. 1996. Structural framework and denudation history of the flanks of the Kenya and Anza Rifts, East Africa. *Tectonics* **15**, 258-271.
- Galbraith, R. F. 1990. The radial plot: Graphical assessment of spread in ages. *Nuclear Tracks Radiation Measurements* **17**, 207-214.
- Galbraith, R. F. and Laslett, G. M. 1993. Statistical models for mixed fission track ages. *Nuclear Tracks Radiation Measurements* **21**, 459-470.
- Gallagher, K. 1995. Evolving temperature histories from apatite fission track data. *Earth Planetary Science Letters* **136**, 421-435.
- Gleadow, A. J. W. and Fitzgerald, P. G. 1987. Uplift history and structure of the Transantarctic Mountains: new evidence from fission track dating of basement apatites in the Dry Valleys area, southern Victoria Land. *Earth Planetary Science Letters* **82**, 1-14.

- Gleadow, A. J. W., Duddy, I. R., Green, P. F. and Lovering, J. F. 1986. Confined fission track lengths in apatite: a diagnostic tool for thermal history analysis. *Contributions Mineralogy Petrology* **94**, 405-415.
- Green, P. F., Duddy, I. R., Gleadow, A. J. W. and Lovering, J. F. 1989a. Apatite fission-track analysis as a paleotemperature indicator for hydrocarbon exploration. In: *Thermal history of sedimentary basins* (Edited by Naeser, N. D. and McCulloh, T. H.) pp181-195. Springer-Verlag, New York.
- Green, P. F., Duddy, I. R., Laslett, G. M., Hegarty, K. A., Gleadow, A. J. W. and Lovering, J. F. 1989b. Thermal annealing of fission tracks in apatite 4. Quantitative modelling techniques and extension to geological timescales. *Chemical Geology (Isotope Geoscience Section)* **79**, 155-182.
- Harkin, D. A. 1955. The geology of the Songwe-Kiwira coal field, Rungwe District. *Geological Survey Tanganyika Bulletin* **27**, 17p.
- Harkin, D. A. 1960. The Rungwe volcanics at the northern end of Lake Nyasa. *Geological Survey Tanganyika, Memoir* **11**, 172p.
- Hurford, A. J. 1990. International union of geological sciences subcommission on geochronology recommendation for the standardization of fission track dating calibration and data reporting. *Nuclear Tracks Radiation Measurements* **17**, 233-236.
- Jackson, J. and Blenkinsop, T. G. 1993. The Malawi earthquake of March 10, 1989: Deep faulting within the East African Rift System. *Tectonics* **12**, 1131-1139.
- Jacobs, L. L., Winkler, D. A., Kaufulu, Z. M. and Downs, W. R. 1989. The Dinosaur Beds of Northern Malawi, Africa. *National Geographic Research* **6**, 196-204.
- Janssen, M. E., Stephenson, R. A. and Cloetingh, S. 1995. Temporal and spatial correlations between changes in plate motions and the evolution of rifted basins in Africa. *Geological Society America Bulletin* **107**, 1317-1332.
- Kilembe, E. and Rosendahl, B. R. 1992. Structure and stratigraphy of the Rukwa Basin. *Tectonophysics* **209**, 143-158.
- King, L. C. 1963. *South African Scenery*. 308p. Oliver and Boyd, Edinburgh, London.
- Kreuser, T., Schradmedei, R. and Rullkotter, J. 1988. Gas-prone source rocks from cratogene Karoo basins in Tanzania. *Journal Petroleum Geology* **11**, 169-184.
- Laslett, G. M., Green, P. F., Duddy, I. R. and Gleadow, A. J. W. 1987. Thermal annealing of fission tracks in apatite 2. A quantitative analysis. *Chemical Geology (Isotope Geoscience Section)* **65**, 1-13.
- Lenoir, J. L., Liégeois, J.-P., Theunissen, K. and Klerkx, J. 1994. The Paleoproterozoic Ubendian shear belt in Tanzania: geochronology and structure. *Journal African Earth Sciences* **19**, 169-184.
- Lutz, T. M. and Omar, G. I. 1991. An inverse method of modeling thermal histories from apatite fission-track data. *Earth Planetary Science Letters* **104**, 181-195.
- Mbede, E. I. 1993. Tectonic development of the Rukwa Rift Basin in SW Tanzania. *Berliner Geowissenschaftliche Abhandlungen* **A152**, 92p.
- Mbede, E. I., Hurford, A., Ebinger, C. J. and Schandemeier, H. 1993. A constraint on the uplift history of the Rukwa rift, SW Tanzania: a reconnaissance apatite fission track analysis. *Rapport Annuel 1991-1992*, pp99-108. Département de Géologie et Minéralogie, Musée Royal de l'Afrique Centrale, Tervuren, Belgium.
- Morley, C. K., Cunningham, S. M., Harper, R. M. and Wescott, W. A. 1992. Geology and geophysics of the Rukwa rift, East Africa. *Tectonics* **11**, 68-81.
- Noble, W. P. 1997. Post Pan-African tectonothermal evolution of Eastern Africa: An apatite fission track study. *Ph. D. Thesis*. LaTrobe University, Bundoora (Victoria, Australia).
- Noble, W. P., Foster, D. A. and Gleadow, A. J. W. 1997. The Post Pan-African tectonothermal development of the Mozambique belt in eastern Tanzania. *Tectonophysics* **275**, 331-350.
- Nyblade, A. A., Pollack, H. N., Jones, D. L., Podmore, F. and Musjayandevu, M. 1990. Terrestrial heat flow in East and Southern Africa. *Journal Geophysical Research* **95**, 17,371-17,384.
- Omar, G. I., Steckler, M. S., Buck, W. R. and Kohn, B. P. 1989. Fission-track analysis of basement apatites at the western margin of the Gulf of Suez rift, Egypt: evidence for synchronicity of uplift and subsidence. *Earth Planetary Science Letters* **94**, 316-328.
- Ring, U., Betzler, C. and Delvaux, D. 1992. Normal vs. strike-slip faulting during rift development in East Africa: the Malawi rift. *Geology* **20**, 1015-1018.
- Rosendahl, B. R. 1987. Architecture of continental rifts with special reference to East Africa. *Annual Review Earth Planetary Sciences* **15**, 445-503.
- Rosendahl, B. R., Kilembe, E. and Kaczmarick, K. 1992. Comparison of the Tanganyika, Malawi, Rukwa and Turkana rift zones from analyses of seismic reflection data. *Tectonophysics* **213**, 235-256.
- Semkiwa, P. Z. 1992. Depositional environments and coal petrography of Permian coal deposits of SW Tanzania. *Geologisches Institut Universität Köln Sonderveröffentlichungen* **84**, 184p. Cologne, Germany.
- Ter Voorde, M. and Cloetingh, S. 1996. Numerical modeling of extension in the faulted crust: effects of localized and regional deformation on basin stratigraphy. In: *Modern Developments in Structural Interpretation, Validation, and Modelling* (Edited by Buchanan, P. G. and Nieuwland, D. A.) *Geological Society Special Publication* **99**, 283-296.
- Theunissen, K., Lenoir, J.-L., Liégeois, J.-P., Delvaux, D. et Mruma, A. 1992. Empreinte mozambiquienne majeure dans la chaîne ubendienne de Tanzanie sud-occidentale: géochronologie U-Pb sur zircon et contexte structural. *Comptes Rendus Academie Sciences Paris, Série II* **314**, 1355-1362.
- Theunissen, K., Klerkx, J., Melnikov, A. and Mruma, A. 1996. Mechanisms of inheritance of rift faulting in the western branch of the East African Rift, Tanzania. *Tectonics* **15**, 776-790.
- Tiercelin, J.-J., Chorowicz, J., Bellon, H., Richert, J.-P., Mwambene, J. T. and Walgenwitz, F. 1988. East African rift system: offset, age and tectonic significance of the Tanganyika-Rukwa-Malawi intracontinental fault zone. *Tectonophysics* **148**, 241-252.
- Upcott, N. M., Mukasa, R. K., Ebinger, C. J. and Karner, G. D. 1996. Along-axis segmentation and isostasy in the Western rift, East Africa. *Journal Geophysical Research* **101**, 3247-3286.
- Van den Haute, P. 1984. Fission-track ages of apatites from the Precambrian of Rwanda and Burundi: relationship to East African rift tectonics. *Earth Planetary Science Letters* **71**, 129-140.
- Van der Beek, P. A. 1995. Tectonic evolution of continental rifts: Inferences from numerical modelling and fission track thermochronology. *Ph. D. Thesis* 248p. Vrije Universiteit Amsterdam, the Netherlands.
- Van der Beek, P. A., Cloetingh, S. and Andriessen, P. A. M. 1994. Mechanisms of extensional basin formation and vertical motions at rift flanks: Constraints from tectonic modelling and fission-track thermochronology. *Earth Planetary Science Letters* **121**, 417-433.

- Van der Beek, P. A., Delvaux, D., Andriessen, P. A. M. and Levi, K. G. 1996. Early Cretaceous denudation related to convergent tectonics in the Baikal region, SE Siberia. *Journal Geological Society London* **153**, 515-523.
- Versfelt, J. and Rosendahl, B. R. 1989. Relationships between pre-rift structure and rift architecture in Lakes Tanganyika and Malawi, East Africa. *Nature* **337**, 354-357.
- Wagner, G. A. 1979. Correction and interpretation of fission track ages. In: *Lectures in Isotope Geology* (Edited by Jäger, E. and Hunziker, J. C.) pp170-177. Springer Verlag, Berlin.
- Wagner, M., Altherr, R. and van den Haute, P. 1992. Apatite fission-track analysis of Kenyan basement rocks: constraints on the thermotectonic evolution of the Kenya dome. A reconnaissance study. *Tectonophysics* **204**, 93-110.
- Weissel, J. K. and Karner, G. D. 1989. Flexural uplift of rift flanks due to mechanical unloading of the lithosphere during extension. *Journal Geophysical Research* **94**, 13919-13950.
- Wescott, W. A., Krebs, W. K., Engelhardt, D. W. and Cunningham, S. M. 1991. New biostratigraphic age dates from the Lake Rukwa rift basin in Western Tanzania. *American Association Petroleum Geologists Bulletin* **75**, 1255-1263.
- Wheeler, W. H. and Karson, J. A. 1989. Structure and kinematics of the Livingstone Mountains border fault zone, Nyasa (Malawi) Rift, southwestern Tanzania. *Journal African Earth Sciences* **8**, 393-413.
- Wheeler, W. H. and Karson, J. A. 1994. Extension and subsidence adjacent to a "weak" continental transform: an example of the Rukwa Rift, East Africa. *Geology* **22**, 625-628.
- Wopfner, H. 1990. Rifting in Tanzanian Karoo basins and its economic implications In: *Etudes Récentes sur la Géologie de l'Afrique, 15e colloque de Géologie Africaine, Nancy 1990* (Edited by Rocci, G. and Deschamps, M.) *CIFEG Occasional Publications* **1990/22**, 217-220.
- Wopfner, H. 1993. Structural development of Tanzanian Karoo basins and the break-up of Gondwana. In: *Gondwana Eight; Assembly, Evolution and Dispersal* (Edited by Findlay, R. H., Unrug, R., Banks, M. R. and Veevers, J. J.) pp531-540. Balkema, Rotterdam.